

Chapter 4

Acrylic Acid (AA) Based Polyaniline Composite for Liquefied Petroleum Gas (LPG) Sensors

Muktikanta Panigrahi ^{1,*}, Basudam Adhikari ¹

¹ Materials Science Centre, Indian Institute of Technology, Kharagpur, West Bengal, India

*Corresponding author: muktikanta2@gmail.com

Abstract

N-substituted PANI-ES was obtained from N-phenyl- β -alanine (N-substituted aniline). N-phenyl- β -alanine was synthesized chemically from methyl acrylate and aniline precursor. ESI-MS, ¹H NMR spectroscopy and FTIR spectroscopy are employed to characterise the N-phenyl- β -alanine for structure elucidation. The structure and properties of corresponding polymers were investigated by X-ray diffraction, FTIR, UV-Visible, ¹H NMR, FESEM, solubility, and DC conductivity. On the basis of experimental results of prepared N-substituted aniline monomer and its corresponding polymer is proposed. At room temperature, the average DC conductivity of as-prepared PANI polymers was found in semiconducting range, which is 0.153 S/cm for poly (3-methyl (phenyl amino) propionic acid). We also were analysed temperature dependent DC conductivity with and without magnetic field of as prepared PANI polymers to understand the conduction mechanism and it was followed variable-range hopping (VRH) process. In addition, we were discussed the response of liquefied petroleum gas (LPG) with polyaniline based sensor materials.

Keywords: Dopant, Amorphous, Electrical conductivity, Conduction mechanism, Thermal stability, Solubility

1.0 Introduction

Now days, scientific communities have taken much more interest towards electronically conducting polymers due to their potential applications in emerging fields such as rechargeable batteries, electrochromic windows, biosensor and antistatic coating materials [1-6]. Particularly, PANI is an important conducting polymer in the conducting polymeric group because of its ease of synthesis *via* chemical and

© IOR INTERNATIONAL PRESS, 2021

Muktikanta Panigrahi & Basudam Adhikari, *Acrylic Acid (AA) Based Polyaniline Composite for Liquefied Petroleum Gas (LPG) Sensors*

<https://doi.org/10.34256/ioriip2124>

electrochemical routes, good environmental stability, unique oxidation reduction chemistry and low cost synthesis, etc [7-9]. However, the conducting form of PANI is insoluble in common organic solvents even in N-methyl-2-pyrrolidone (NMP) and dimethyl sulphoxide (DMSO). The limitation has impeded not only its practical applications but also a complete understanding of the polymer structure [10]. To solve this problem, researchers are devoted to improve the processability, solubility and electronic properties of PANI for their performance. Great effort has been devoted to design acid doped polymer to improve their solubility and processability by the development of synthetic route. Generally, organic and inorganic acid dopants are used in the conducting polymers. These are small molecules and can evaporate at room or higher temperature which affects the conductivity of the PANI. The limitation can be overcome by using bigger size dopants, polymeric acid dopants, and substituted form in conducting PANI polymeric backbone. In case of polymeric acid dopants, the dopant has lower glass transition temperature (T_g) (lower than that of PANI) and then can enhance the flexibility of the PANI film. There are several reports on polymeric acids dopants. These are mentioned as poly (ethenesulfonic acid) [10], poly (acrylic acid) [10,11], poly (styrene sulfonic acid) [10-14], poly (2-(acrylamido)-2-methylpropanesulfonic acid) [15], and poly (amic acid) [16]. These dopants can be used during the synthesis by chemical or electrochemical polymerization of aniline in aqueous solution through oxidative polymerization method [17,18]. Due to the presence of protonic acid groups on polymer chains of the polymeric dopant and to the conformational hindrance created by the flexible chain, it is expected that not all of the acid groups are capable of doping PANI and there should be nonuniform distribution. Consequently, the experimental results of the polymeric acid doped PANI should be different from that of non polymeric protonic acid doped PANI [17,18].

Substitution at nitrogen of PANI backbone is another kind to assist the improvement of processability along with hydrophilicity and compatibility. Several reports show that alkyl group-, alkyl ring- are attached to N-atom of PANI. The polymers have been formed directly from aniline monomers, which are soluble in common organic solvents [19,20]. Incorporation of the side groups into PANI has changed its properties. Other than the above approach, co-polymerization of aniline with suitable substituted aniline to produce co-polymers is possible to improve its solubility in organic solvents [21,22]. Utilizing a functionalized acid, *e.g.*, dodecyl benzenesulphonic acid or 10-camphorsulphonic acid, to protonate the base form of PANI improved the processability [23].

Doped conjugated polymers exhibit characteristic properties of the metallic state, which is showing high electrical conductivity. Usually, highly doped conducting polymers do not show the metallic transport, *i.e.*, resistivity (ρ) is not proportional to the temperature. Now a days, the quality of the conjugated polymers has been improved by doping process and results the in-homogeneity in the doping level. Also, the processability has assisted to enhance the quality of conjugated polymer. The doped conjugated polymeric chains are often disordered and structurally amorphous. In the conjugated polymer, some regions are crystalline and other regions are amorphous in nature. The amorphous regions can dominate the electrical transport.

Consequently, the characteristic metallic features in the bulk electrical transport properties are severely limited by strong disorder [24].

Presence of partially filled bands in the doped polymers, the electronic structure will be the similar to that of metal. It is well known that disorder can result in localization of states. If all states become localized, the system will be an insulator. In such an insulator, there is no gap in the density of states, *i.e.*, Fermi level (E_F) lies in an energy interval in which all states are localized, called Fermi glass. In this system, the conductivity is influenced by temperature. At high temperatures, the activation energy is measured by the energy difference between E_F (which lies in the region of localized states) and the mobility edge and at lower temperatures, variable-range-hopping (VRH) transport is resulted from the existence of unoccupied localized electronic states near E_F . Transition from metal to insulator (M-I) occurs when the disorder is sufficiently weak that means mobility edges move away from the center of the band toward the band tails such that E_F lies in a region of extended states. To understand the transport phenomena of conducting polymer, it is important to quantify the disorder by estimating/calculating the transport parameters and to establish the M-I transition [24].

Several reports are found on transport phenomena of conducting polymers. Li and co-workers [25] proposed a variable range of hoping (VRH) model which described the transport mechanism of HCl doped and DBSA doped PANI. Kapil *et al.* [26] analyzed transport mechanism of p-toluene sulphonic acid (PTSA) doped PANI by Arrhenius model, Variable range hoping (VRH) model and Kivelson model in the temperature range of 30-300K. The conduction mechanism of PANI organic film and metal particles embedded in an insulating material and PANI was also explained by using VRH and charge energy limited tunnelling (CELT) models [26]. The conductivity measurements were also done in the presence of magnetic field to measure the magnetoresistance (MR). Several conducting polymers such as PANI [24,26-31], polypyrrole [32-34], PEDOT films [35], and PANI composites have shown positive MR at low temperature (<10 K).

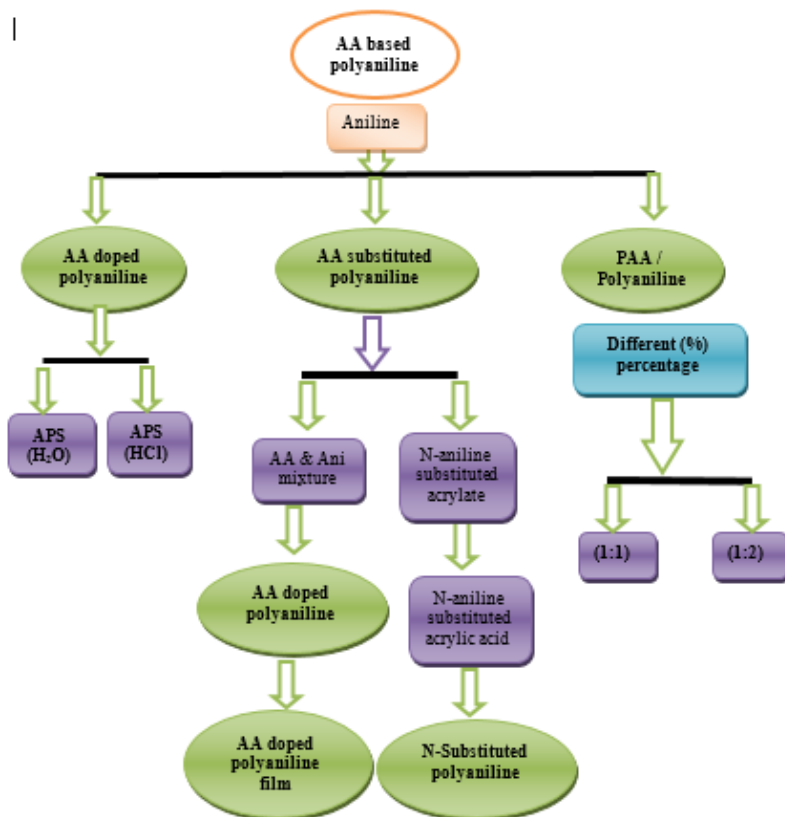
This work was undertaken to study the synthesis, spectroscopic analysis, measurement of electronic properties, microstructure and thermal stability of the AA doped, substituted AA and polymeric protonic acid, *i.e.*, PAA/PANI. Its electronic properties at the temperature range and optical band of the doped PANI were also investigated. Acrylic acid is taken as three forms, *viz.*, doped form, substituted form, polymeric form, *i.e.*, PAA. We present the results of a comprehensive study of the transport in AA based PANI polymer. In the system, DC conductivity as a function of temperature and resistivity in the presence of magnetic field was studied in temperature range 70-300 K. We have observed variable-range-hopping behaviour due to the presence of extent of disorder in the prepared materials. Magnetic fields of 0.4 T induced a transition from the critical regime of M-I transition to the insulating region where the states near E_F are localized and the transport took place *via* variable-range hopping. Various transport parameters of AA based PANI polymers were calculated for understanding the conduction mechanism. An understanding of the

system should also be applicable to systems with other polymeric protonic acid dopant and would provide valuable information for applications of the doped PANI in different applications like electromagnetic interference shielding, in conductive coatings, and as positive electrodes of electroluminescence diode.

2.0 Experimental

2.1 Synthesis of AA Based Pani Polymer

Materials. Acrylic acid (AA), aniline (Ani), dichloromethane (DCM), ammonium persulfate (APS), N,N-dimethyl formamide (DMF), Dimethylsulphoxide (DMSO), methyl acrylate, sodium hydroxide (NaOH), n-hexane, and HCl, ethyl acetate were procured from Merck. All the chemicals are synthesis grade. Distilled water is used in the synthesis.



Scheme 1. Design of AA based polyaniline: AA doped polyaniline, substituted PANI and PAA/PANI composite

Synthesis of AA based PANI polymer. The design of AA based PANI polymer is mentioned as follows in **Scheme 1**. In the synthesis **Scheme 1**, acrylic acid

used in three different ways *viz.*, AA is used as doping in the synthesis of PANI polymer [36], AA is employed as substitution on N-atom (NH₂) of aniline, called monomer [37] and it is polymerised to form the PANI [38]. N-substituted aniline monomers was synthesised in two ways *viz.*, one is direct mixing of AA and aniline and another way of synthesis was used the reference 37. PAA and PANI are used during the preparation of PAA/PANI composite [38]. The design of AA based polyaniline is presented in **Scheme 1**. We have employed chemical routes to synthesize acrylic acid (AA) based PANI polymer. The details synthesis procedures have been described.

Synthesis of acrylic acid (AA) based PANI polymer

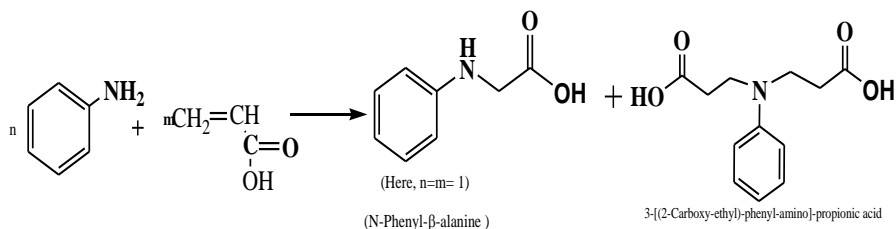
Synthesis of acrylic acid (AA) doped PANI from aniline precursor. AA doped PANI was synthesised following the method in literature [36] and occurred by chemical oxidation process. In this method, AA (2 mL) was added to 50 mL of distilled water and stirred slowly to form AA solution. Then, aniline (2.66 mL) was added slowly to AA solution in stirring condition. Before addition of APS, temperature of system was maintained at 5 °C with continuous stirring. Then, an aqueous solution of APS (2.76 g in 50 mL of distilled water) was added slowly to the above AA solution for 1 h under continuous stirring. The polymerization reaction was carried out. During the polymerization, slight green precipitate was formed in initial stage of polymerization and green precipitate was formed when polymerization proceeds which is followed to stand overnight to complete the polymerization. After filtration, the precipitate was washed adequate amount of distilled H₂O till the precipitate becomes neutral. This washing step removed the unreacted AA and APS. The product was dried under vacuum at 60 °C for 12 h. After that, the solid mass was grinded using mortar and pastel and finally, we got powder. Schematically, the flow chart for synthesis of AA doped PANI polymer is presented in **Scheme 2**.



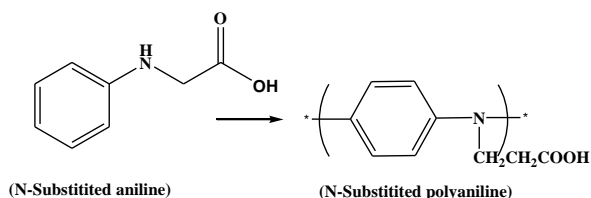
Scheme 2. Schematic flow chart for the synthesis of AA doped PANI polymer

Synthesis of N-substituted aniline monomer and N-substituted PANI polymer from aniline (Ani) and AA/methyl acrylate precursors. Initially, N-substituted aniline monomer was synthesized using AA and Ani predecessors and then

it was polymerizes by chemical-oxidation method. Equivalent amount (mili-equivalent) of both colorless liquid **Ani** and **AA** were mixed together with continuous (45 min) stirring at 5 °C. At last, colorless viscous mixture was formed with the evolution of heat. The reaction was exothermic in nature. During the reaction, different color transitions were observed. The obtained mass became viscous, the color of which changed from colorless to light pink then to light greenish-yellow. Such viscous mass was purified using co-precipitation technique. At first, the mixture was dissolved in dichloromethane (**DCM**) followed by n-hexane in the ratio 1:5. It was preserved in a refrigerator for 12 h. After that, the mass formed two layers in the flask (gel in bottom part and liquid in upper part). The upper liquid part was discarded carefully. Appropriate amount of water was added to the prepared gel and shacked for 15 min. **APS** (0.045 moles) as oxidant was dissolved in 60 mL of water to make oxidant solution. The oxidant solution was added drop wise into deep-end of the purified gel solution through injection syringe with continuous stirring. At this stage, temperature was maintained (10 to 0 °C) using ice bath. After 2 h, the reaction mixture was brought to room temperature in stirring condition for 10 h more. The change of color of the solution was observed, which was from colorless to deep greenish and the polymer was formed as deep green solid lump, which is floated on the solution. The solid polymer was dissolved in **DMF** and distilled water was poured into the solution from which the polymer precipitated out and thus we got polymer without any inorganic impurity. From the spectroscopic analysis is confirmed the formation of mixture of monomer. Accordingly, the reaction Scheme for synthesis of prepared monomer and its corresponding polymer are shown in **Schemes 3** and **4**, respectively.



Scheme 3. Synthesis of mixture of N-substituted aniline monomer

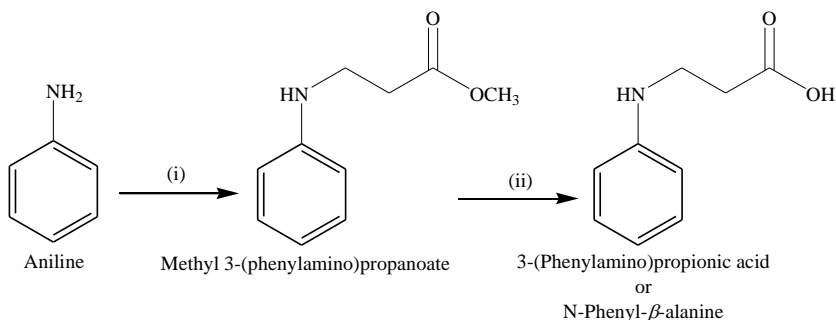


Scheme 4. Synthesis of N-substituted polyaniline

Our aim was to synthesize 3-methyl (phenylamino) propanoic acid (N-Phenyl- β -alanine), which is 100% abundance. This was used to polymerize to form poly (3-methyl (phenylamino) propanoic acid). Poly (3-methyl (phenylamino)

propanoic acid) was further used for different characterizations and analysis. 3-methyl (phenylamino) propanoic acid was synthesized as reported earlier [37]. It is a two step reaction: aniline was first converted to β -amino ester (**Scheme 5**). For this synthesis, 1.623 g aniline (17.43 mill mole) was added slowly to 1.5 g methacrylate (17.43 mill mole) in 6 mL of dry toluene. HCl-treated MMT (0.3 g, 10 wt%, used as catalyst) was added to the reaction mixture. The reaction was carried out in dry condition. The reaction temperature was maintained at 90 °C using oil bath and was continued for 2 h with vigorous stirring. During the reaction, the transition of color of compound was observed from colorless to light brown. Finally, the solvent was evaporated using rotary evaporator to obtain a densed brown product, methyl 3-(phenylamino) propionate. Without further purification, the crude product was used for the next step.

In the second step, the synthesized 3-methyl (phenylamino) propanoate was converted to 3-methyl (phenylamino) propanoic acid (β -amino acid) (**Scheme 5**). For this, 2.89 g (17.49 mill mole) β -amino ester was added to 10 mL methanol in a round bottom flask, followed by the addition of 0.699 g NaOH (17.49 mill mole). The reaction mixture was stirred vigorously for 2 h and the temperature was maintained at 05 °C using ice-bath. After that, methanol was evaporated using vacuum rotary evaporator to get viscous mass. The product was neutralized by the addition of 6 M HCl in cold condition and the pH was adjusted to ~4. Finally, the product was extracted with ethyl acetate several times. Then the solvent was evaporated using vacuum rotary evaporator. The product was precipitated using n-hexane. The product was dried under vacuum to obtain light brown mass. Reaction Scheme for synthesis single N-substituted aniline monomers is presented in **Scheme 5**.



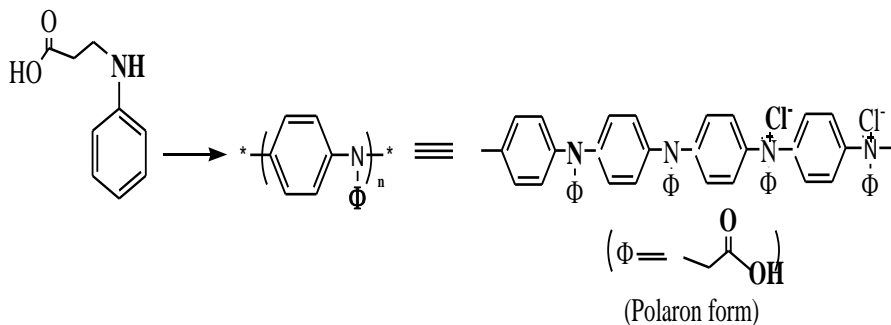
Reagent and conditions:

(i) Methyl acrylate, Toluene, 90 °C, 2 h; (ii) MeOH, NaOH, 0-5 °C, 2 h

Scheme 5. Synthesis of 3-methyl (phenylamino) propanoate and 3-methyl (phenylamino) propanoic acid single monomer

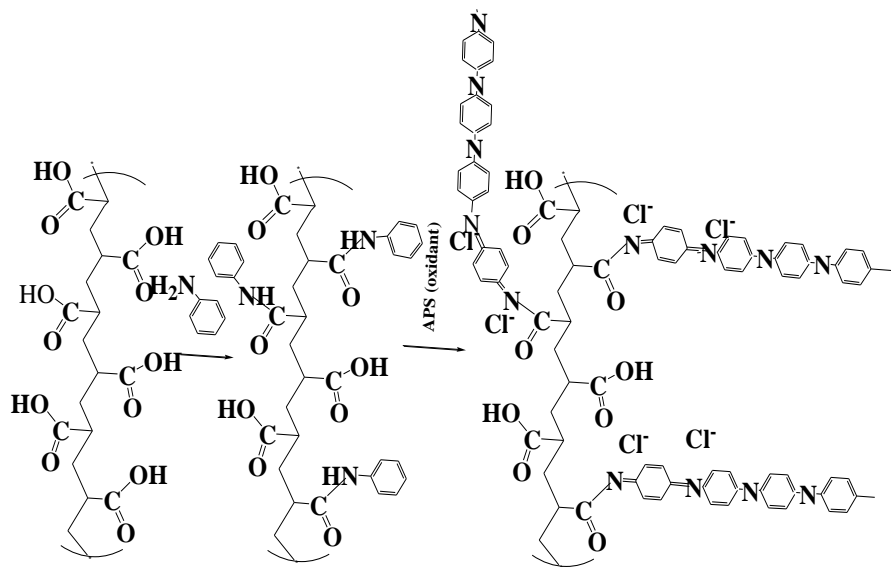
The nanostructures of poly (3-methyl (phenylamino) propanoic acid) doped with HCl were synthesized by a chemical oxidation method. Poly (3-methyl (phenylamino) propanoic acid) doped with HCl was synthesized as follows: Aniline (0.165 g) was mixed with in 10 mL distilled water in the ice bath to form N-substituted aniline solution. Then, an aqueous solution of APS (0.001 mol) in 25 mL of 0.01 M

HCl solution was added drop wise to the above solution. The polymerization was carried out for 12 h in the ice bath. A green solid of HCl doped poly (3-methyl (phenylamino) propanoic acid) was obtained after rinsing with H₂O, CH₃OH, and CH₃OCH₃ for three times [38]. The reaction scheme for synthesis of HCl doped poly (3-methyl (phenylamino) propanoic acid) polymers are shown in following **Scheme 6**.



Scheme 6. Synthesis of HCl doped poly (3-methyl (phenylamino) propanoic acid)

Synthesis of PAA/PANI composites. The **PAA/PANI** composites were prepared by chemical oxidation process in aqueous medium [38]. The **PANI/PAA** composites were prepared as follows: aniline was added to the **PAA** (commercially available, $M_w \sim 1800$) solution with constant stirring at room temperature and solution becomes colorless.



Scheme 7. Reaction scheme for synthesis of HCl doped **PAA/PANI** composite

The ratio **PAA** and aniline was 1.0:0.5 (w/w). Next, the reaction mixture was

cooled to 5 °C and stirred for 1 h. During this time, freshly prepared APS solution (0.01 mol APS in 0.001 M HCl) was added slowly to the reaction mixture. After 2 h, the mixture was brought to the room temperature and stirred continuously for 6 h to complete the polymerization of aniline. The color of the mixture changed from colorless to deep green. The obtained product was kept 12 h for complete the polymerization after which the polymer was filtered with Buckner funnel. After that, these products were washed with distilled water several times (pH ~7) and dried under vacuum at 60 °C for 6 h to get composites. The reaction for synthesis of HCl doped PAA/PANI polymer is presented in **Scheme 7**.

2.2. Characterization Techniques

FTIR spectra were recorded on a Thermo Nicolet Nexus 870 spectrophotometer in the range 400-4000 cm^{-1} . The instrument settings were kept constant (50 scan at 4 cm^{-1} resolution, transmittance mode). **Ani, AA, AA and Ani mixture, β -amino acid, PAA and AA based PANI samples** were used. Before running the samples, a background spectrum was collected. Then samples were put in a sample holder and data were collected. **$^1\text{H-NMR}$** of AA and Ani mixture, **β -amino acid** and its **corresponding polymer** are recorded using **Bruker DRX500 MHz** spectrometer at IIT Kharagpur (Chemistry Dept.). These were dissolved separately in **$\text{d}_6\text{-DMSO}/\text{CDCl}_3$** and **$\text{CDCl}_3$** . The chemical shifts of the groups are recorded in the range 10-200 Hz for monomer and 10-400 Hz for prepared polymer with a delay of 2.5 sec. Identification of the product ions formed during **ESI-MS** analyses were performed on **AXIMACFR** laser desorption ionization flying time spectrometer (**COMPACT**). In order to identify these product ions, structure of prepared compound were created. Gel as well as solid granules materials were analysed and are fine aerosol. It helps to evaporate solvent easily. Typical solvents for electrospray ionization are prepared by mixing water with volatile organic compounds like methanol and acetonitrile. Acetic acid is added to prepared typical solvent. X-ray diffraction (**XRD**) experiments were performed using a Phillips PW-1710 Advance wide angle X-ray diffractometer, **Phillips PW-1729** X-ray generator, and Cu $K\alpha$ radiation (wavelength, $\lambda = 0.154 \text{ nm}$). The generator was operated at 40 kV and 20 mA. The powder samples were placed on a quartz sample holder at room temperature and were scanned at diffraction angle 2θ from 5° to 60° at the scanning rate of 2 °/min. Acrylic acid based PANI samples was taken for XRD analysis. The **UV-Visible** spectra of aniline, acrylic acid, acrylic acid based monomers and its corresponding polymer(s) were recorded by using a **Micropack UV-VIS-NIR, DH 2000** in the wavelength region 200-800 nm. The samples were dissolved in N-methyl pyrrolidone (**NMP**). Base line was corrected before recording the spectra. This technique was performed for studying the variety of electronic transitions. Surface morphologies of acrylic acid based PANI polymer as well as N-substituted aniline (monomer) were analyzed by field emission scanning electron microscopy (**FESEM**) using **Carl Zeiss Supra 40** scanning electron microscope. Before FESEM experiment, gold coating was needed. Operating voltage was 4 kV. The enthalpy of fusion of prepared AA based PANI polymer was calculated from differential scanning calorimetry (**DSC**)

experiment. The parameters such as heating rate = 10 °C/min, temperature range = 50 to 350 °C were set. The thermal stability of the prepared materials was determined by thermogravimetric (TG) analysis using a NETZSCH TG-209 F1 analyzer at a heating rate of 10 °C/min in nitrogen environment from 50-700 °C.

The room temperatures as well as temperature dependent DC conductivity of the prepared acrylic acid based PANI polymer were measured using linear four-probe technique. Four contacts were made with nonconducting silver paste.

A constant current (I) from a current source (Keithley 2400 programmable current source) was allowed to pass through two terminal leads of the four probe and the voltage (V) across the other two leads was measured using a multimeter (Keithley 2000 digital multimeter). According to four point probe method, the resistivity (ρ) was calculated using the relation [39]

$$\rho = 2\pi S \left(\frac{V}{I} \right) \dots\dots\dots (1)$$

where S is the probe spacing in centimetres (cm), which was kept constant, (I) is the supplied current in mill-amperes (mA) and the corresponding voltage (V) was measured in mili-volts (mV). The conductivity (σ) was calculated using the relation as follows [39]

$$\sigma = \frac{1}{\rho} \dots\dots\dots (2)$$

For temperature variation resistivity measurement, the chamber pressure was maintained at 10⁵ torrs. The Lakeshore (model 331) temperature controller was connected. Then, we measured DC resistivity. A constant current is passed through the two side probes and measured voltage in the two middle probes. A DC current source (Keithley 220 programmable) was taken. Different millampere/nanoampere current was applied and corresponding voltage was measured. Voltage across the terminals was measured using Keithley nanovoltmeter (model 2182). For In addition, the resistivity measurement with a particular magnetic field is a function of temperature which is important for calculating localisation length (L_{loc}). Determination of other different transport parameters [28] such as Density of states at Fermi level ($N(E_F)$), Motts characteristics temperature in Kelvin (T_{Mott}), Mott’s hoping distance ($R_{Hop, Mott}$ in nm at 300 K) and the energy difference ($\Delta_{Hop, Mott}$) between the sites in the Mott’s limits is calculated using L_{loc} . These are the important parameters to understand the conduction mechanism.

2.3. Results And Discussion

The outcomes obtained from different experiments of monomer synthesis

and polymerizations are described separately.

Monomer synthesis

The mixture of aniline and acrylic acid (gel-like monomer) was purified using DCM and n-Hexane solvents. The purpose was to remove excess of unreacted monomers. Such process is called co-precipitation method. Particularly, for this monomer synthesis, colorless liquid aniline (2 mL) was added directly on colorless acrylic acid (2 mL) to form impure monomer. During the formation, a different color was observed as shown in **Fig. 1**. There may be an interaction between the two materials. The excesses individual precursors were removed using precipitation technique. Impure monomers were dissolved by DCM and followed by n-Hexane. Such solution was kept at low temperature (0-5 °C) for 12 h. The purpose of using DCM and n-Hexane was to remove excess of precursors. Color transition during the preparation of gel like monomer is shown in **Fig. 1**.

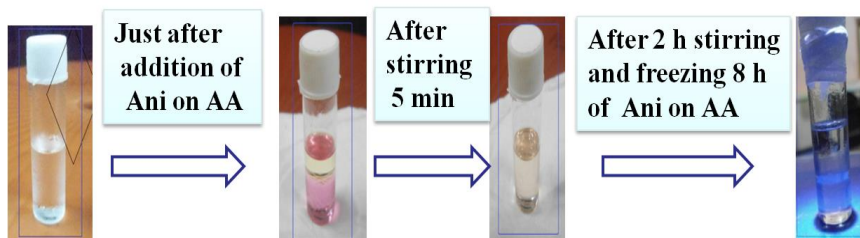


Figure 1. Color change during the synthesis of N-substituted anilinic monomer (aniline and acrylic acid mixture)

For the synthesis of N-Phenyl- β -alanine, aniline and methyl acrylate were taken in dry toluene [36]. HCl-treated MMT was used as catalyst to the reaction mixture. The reaction was carried out in dry condition. The reaction temperature (90 °C) was maintained using an oil bath. During the reaction, the transition of color was observed from colorless to light brown. After solvent evaporation, a dense brown product was obtained. This product was used for the next step. For the conversion of ester to acid, crude product (prepared from first step) was added to methanol followed by addition of NaOH and 6 M HCl. Finally, the product was extracted with ethyl acetate several times. After solvent evaporation, precipitation by n-hexane and drying, a light brown mass was obtained.

ESI-MS, H^1 NMR, and FTIR techniques were used for structural elucidation of substituted aniline monomer.

ESI-MS analysis

For structural analysis, the masses of adducts formed from these compounds via the attachment of various different species ($[P + (M)n]n+$, where P represents a target compound; M represents a solvent molecule or sodium, potassium, lithium,

silver, hydrogen, or ammonium cations; and $n = 1$ for singly charged ions or $n = 2$ for doubly charged ions) were calculated [37]. The exact masses calculated for these adduct species are used in the assignment of peaks generated in the ESI-MS experiments. To assign chemical structures of acrylic acid and aniline mixture, 3-methyl (phenyl amino) propanoate and 3-methyl (phenyl amino) propionic acid were investigated by ESI-MS and it is presented in **Fig. 2, 3** and **4**. The spectra were generated using the normal scan mode. The spectra were taken (zoom scan) over representative m/z areas of the region dominated by ideal star peaks (**Fig. 2, 3** and **4**). In **Fig. 2**, by comparing theoretical m/z values to these peaks, the adduct species are able to be found and these are mechanistically feasible. In **Fig. 2**, the observed m/z value of small peak (below 100 % abundance) matches with the theoretical m/z of hydrogen adducts formed from the products (substituted anilinic monomer obtained from aniline and acrylic acid) and most intense peak (100%) corresponds to hydrogen adducts of N,N-disubstituted anilinic product (100 % abundance). Other than these peaks, a significant number of non-reproducible and/or non-periodic peaks were observed in these spectra, which were not unexpected. Thus, it is not mechanistically feasible and disregarded.

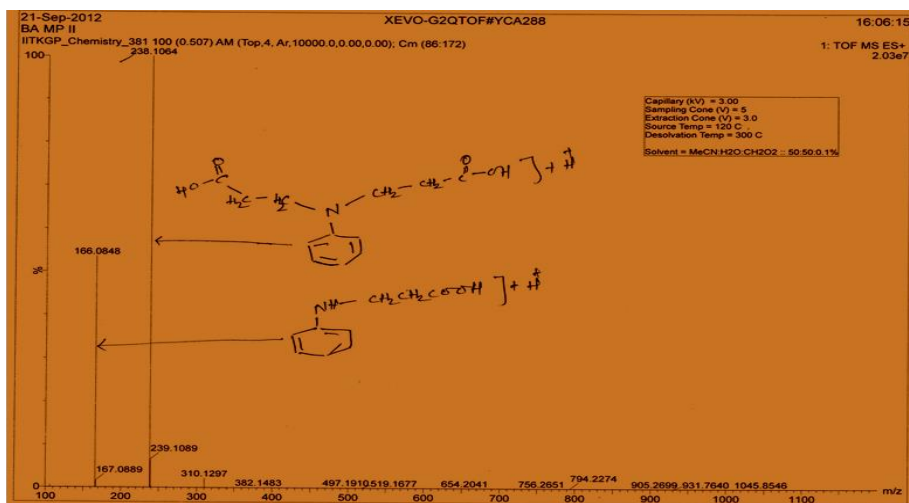


Figure 2. ESI-MS spectrum of monomer obtained from AA and Aniline mixture

In **Fig. 3**, 100 % abundant peak matched with hydrogen adduct, which has arisen from 3-methyl (phenyl amino) propionate product (mentioned the chemical structure of product). No oxidation products are formed. The assignment is mechanistically feasible. Other peaks in the spectrum (**Fig. 3**) are not matched to any adducts. Thus, it can be seen that there is an ambiguity in the assignment of products.

Also, ESI-MS technique is used to characterize the 3-methyl (phenyl amino) propionic acid. In **Fig. 4**, we observed single peak, which is 100% (relative abundance). This peak indicates to 3-methyl (phenyl amino) propionic acid adduct. No oxidation products are formed. The assignment is mechanistically feasible. Other

peaks in the spectrum are not matched to any adducts.

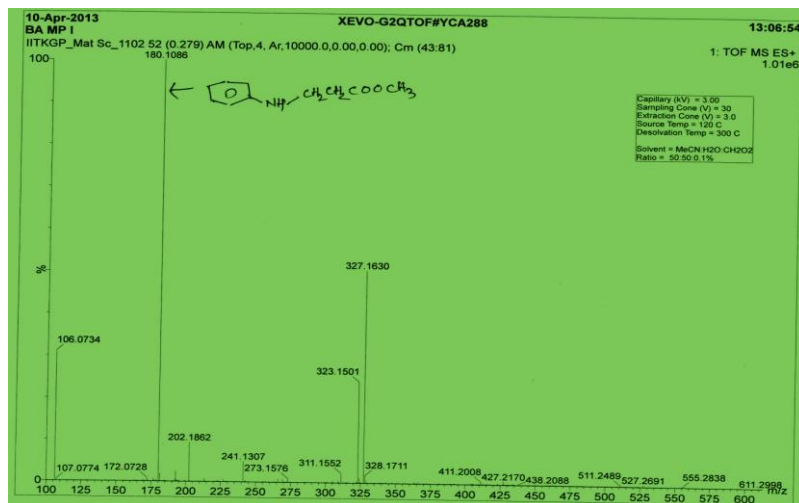


Figure 3. ESI-MS spectrum of anilinic monomer (3-methyl (phenyl amino) propionate) prepared from methyl acrylate and aniline

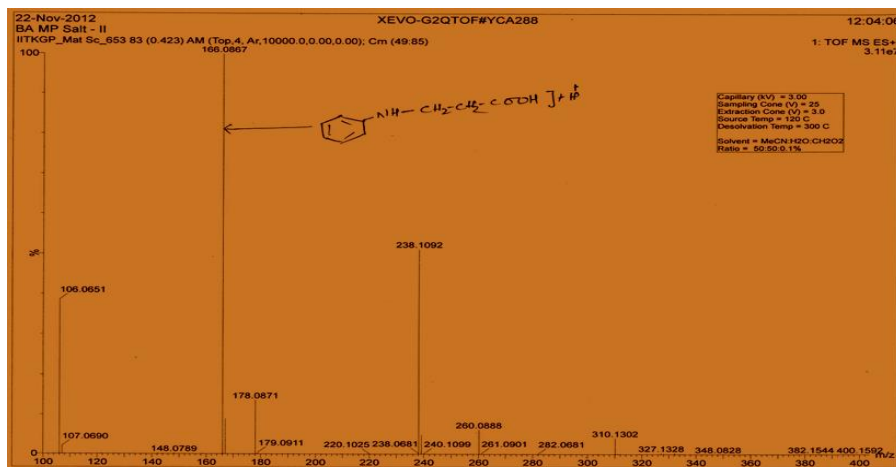


Figure 4. ESI-MS spectrum of 3-methyl (phenyl amino) propionic acid monomer obtained from 3-methyl (phenyl amino) propionate

H¹NMR analysis

Spectroscopic characterizations such as H¹NMR, FTIR and ESI-MS, etc. were employed to elucidate the chemical structure of materials. Out of them, H¹NMR is one of the important spectroscopic characterizations to explore the molecular

structure. For this characterization, we used samples in solution mode. Because, it is done easily with high accuracy. Spectra of synthesised anilinic monomers are shown in **Fig. 5** and **6**. Detail peak positions and their assignments are also presented in **Table 1**. In ^1H NMR analysis, ^1H NMR integration ratios are sufficiently close to their expected nearest integer values, they arise due to the presence of end groups in the monomers. In anilinic monomer (AA and Ani mixture), the presence of phenyl ring proton [38], amine proton [38], and also ethylenic proton ($-\text{CH}_2-\text{CH}_2-$) are found at $\sim 6.658-6.873$ and $7.094-7.295$, ppm, $\sim 4.336-4.422$ ppm, and $\sim 2.608-2.710$ and $3.444-3.638$ ppm, respectively. The ^1H NMR result predicts complex structure of monomeric product. This fact is verified with FTIR spectrum (**Fig. 7**) and ESI-MS spectrum (**Fig. 4**) supports to the monomeric product. These results are in agreement with the expected structures, *i.e.*, N-substituted aniline.

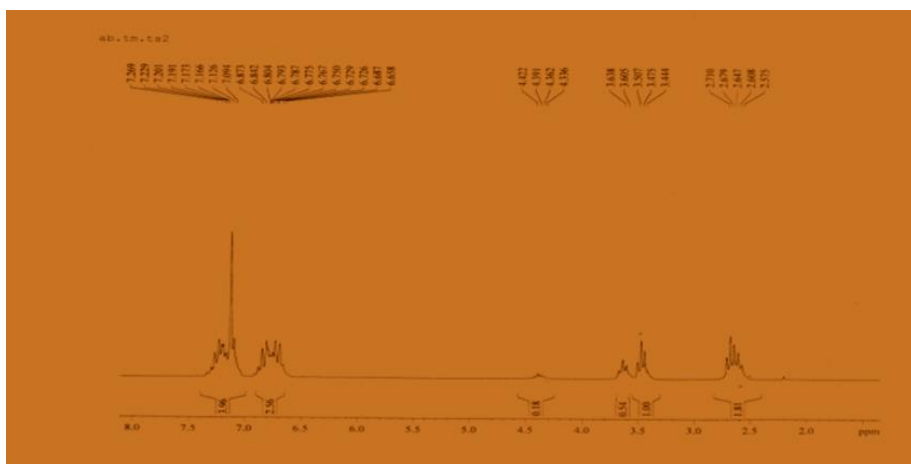


Figure 5. ^1H NMR spectrum of anilinic monomers obtained from AA and Ani. mixture)

In a similar fashion, the 3-methyl (phenyl amino) propionic acid has been characterized by ^1H NMR technique and the spectrum is displayed in **Fig. 6**.

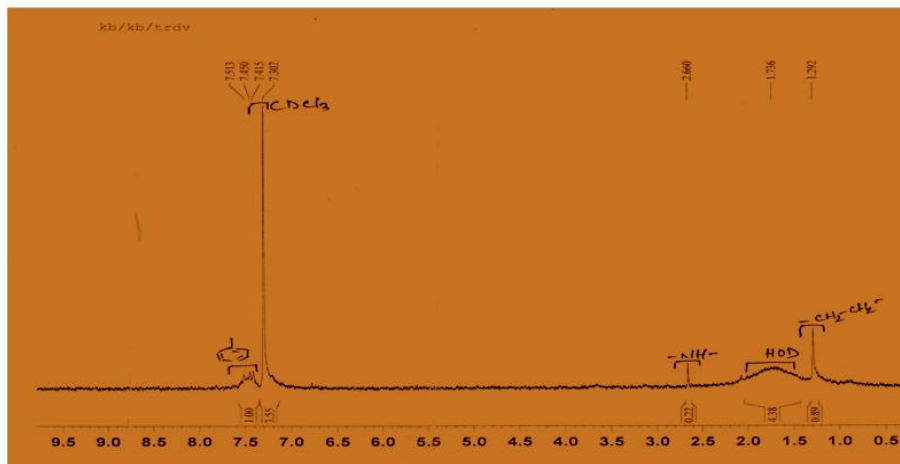


Figure 6. ^1H NMR spectrum of 3-methyl (phenyl amino) propionic acid monomer)

From this spectrum analysis, the peak positions and their assignments are presented in **Table 1**. In **Table 1** various protonic groups such as phenyl protons ($-\text{C}_6\text{H}_5$) at 7.302-7.513 [38], amine proton ($-\text{NH}-$) at 2.66 ppm [38] and ethylenic proton ($-\text{CH}_2\text{CH}_2-$) 1.292 ppm, CDCl_3 (7.3 ppm) [39] were assigned. Thus, it supports a possible structure of repeat unit (3-methyl (phenyl amino) propionic acid).

FTIR analysis

Fig. 7 shows the FTIR spectra of (AA), aniline (Ani) and synthesised anilinic monomers. The characteristic peak positions and their assignments are given in **Table 1**. From **Fig. 7**, the major bands of **AA** at 3062, 1706, 1431 and 1238 cm^{-1} have been attributed to C–H stretching, C=O stretching, and C–O stretching vibration of acid group, respectively [40]. This indicates that the characters of AA are retained. The peaks of **Ani** (**Fig. 7**) are found at 3365, 3034, 1496, and 1173 cm^{-1} corresponding to $-\text{NH}$ -, $-\text{CH}$ -, benzenoid and C=N stretching, respectively [41]. From our observation in **Fig. 7** and **Table 1**, the main bands are $-\text{NH}-$ (3403 cm^{-1}), benzenoid ring (1502 cm^{-1}), $-\text{CH}-$ (2952 cm^{-1}), $-\text{OH}$ (2600 cm^{-1}), $-\text{C}=\text{O}$ (1619 cm^{-1}) and C–O (1241 cm^{-1}), which indicated the presence of both AA and aniline. Also, main bands of prepared substituted monomers of mixture of AA and Ani are found at 3046 cm^{-1} , 1718 cm^{-1} , 3370 cm^{-1} , 1415 cm^{-1} , and 1211 cm^{-1} corresponding to $=\text{C}-\text{H}$ stretching, C=O stretching of ester, N-H stretching, C=C stretching of aromatic ring, C-N stretching, respectively.

Table 1: FTIR, ^1H NMR, and ESI-MS peak positions and their assignments

	Peak positions and their assignments of anilinic monomer from acrylic acid and aniline					
FTIR Peak Positions (cm^{-1})	3403	2952	2600	1619	1502	1241
Its peak assignments	NH	CH	OH	C=O	Benzene ring	=C-N
^1H NMR peak positions	2.575-271	3.444-3.638	4.336-4.422	6.658-6.842	7.094-7.269	
Its peak assignments	CH_2CH_2	NH	impurities	CDCl_3	Benzene proton	
ESI-MS	166	238				

peak positions						
Its peak assignments	N-mono substituted monomer	N,N-di substituted monomer				
FTIR Peak Positions (cm^{-1})	3482	2952	2610	1735	1525	1107
Its peak assignments	NH	CH	OH	C=O	Benzene ring	=C-N
¹ H NMR peak positions	7.3-7.5	7.3	2.6	1.7	1.3	1.0
Its peak assignments	Benzene proton	CDCl_3	NH	HOD	CH_2CH_2	TMS
ESI-MS peak positions	180 (100%)	166	---	---	---	---
Its peak assignments	N-substituted Methyl ester	N-substituted Methyl ester	---	---	---	---

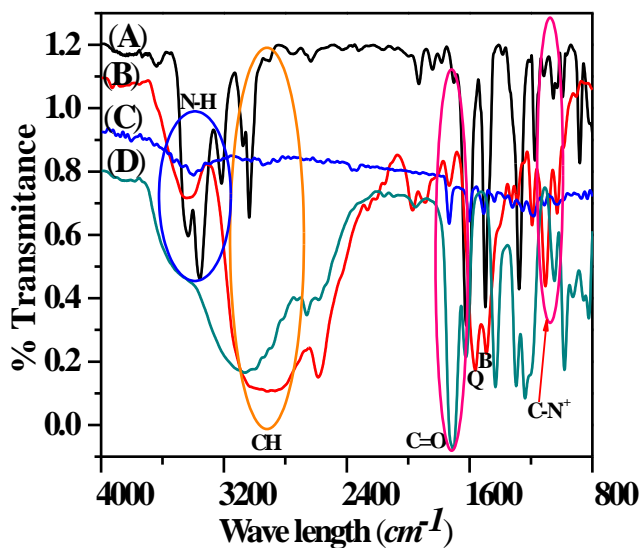


Figure 7. FTIR spectra of Aniline (A), 3-methyl (phenyl amino) propionic acid (B), anilinic monomer (AA and Ani mixture) (C), and AA (D)

Considering the entire peak assignments and peak intensity obtained from the FTIR spectra, the bands of 3-methyl (phenyl amino) propionic acid are found at 2952 cm^{-1} , 1735 cm^{-1} , 3482 cm^{-1} , 1525 cm^{-1} , 2610 cm^{-1} , and 1107 cm^{-1} for C-H stretching, C=O stretching of acid, N-H stretching, C=C stretching of aromatic ring, -OH stretching of carboxylic acid, and C-N stretching, respectively.

XRD analysis

X-ray Diffraction (XRD) was used to study the structure of synthesised 3-methyl (phenyl amino) propionic acid monomeric product and shown in **Fig. 8**. From this **Fig. 8**, we observed sharp peaks, which indicated the crystalline nature of 3-methyl (phenyl amino) propionic acid (monomer) [42].

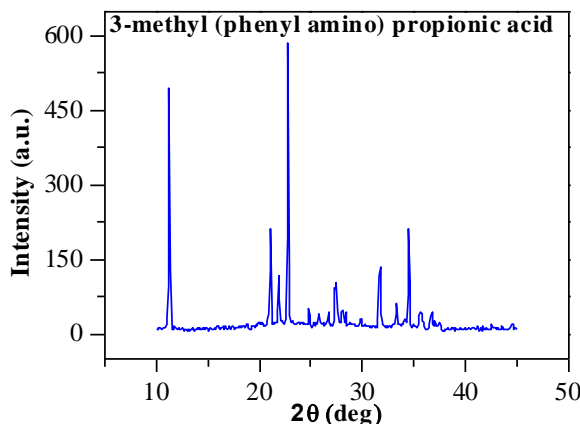


Figure 8. XRD plot of prepared 3-methyl (phenyl amino) propionic acid monomer (methyl acrylate and aniline)

Synthesis of AA based PANI polymer

FTIR, ^1H NMR, UV-Visible, and X-ray diffraction (XRD) spectral analysis of synthesised AA based PANI polymer were done for chemical structure analysis of synthesised AA based PANI.

Synthesis of AA based PANI polymer

For carrying the polymerization, both monomers and oxidant (APS) were taken in water phase. The oxidative coupling polymerizations of the both monomers were mediated at the aqueous medium. As compared to the experimental condition to synthesize substituted PANI, oxidative coupling polymerization was conducted between oxidant and monomers. From FESEM experiment, morphology of

synthesised polymeric product was analysed and it is shown in **Fig. 9**. The FESEM images (**Fig. 9**) show the crystals-like morphology of 3-methyl (phenyl amino) propionic acid, net-like structure of poly (3-methyl (phenyl amino) propionic acid), crystal plates of PAA, cauliflowers like morphology of PAA/PANI composites, globular shapes of AA doped PANI (APS in H₂O), and nanofibers of AA doped PANI (APS in 1 M HCl). In net-like structure, it may be believed that substituted PANI chains are inter-linked, whereas small cauliflowers image shows that PANI chains are interacting with carboxylic group in PAA chains. The interaction is non-uniform. In case of fiber-like morphology, the average diameters of fiber is more than 50 nm, known as nanofiber. Conducting polymers were first nucleated at the interface through oxidative coupling between monomer of PANI and APS (oxidant) in the aqueous layer. These polymers were grown in the aqueous medium. A variety of FESEM images were found in morphology study as shown in **Fig. 9**.

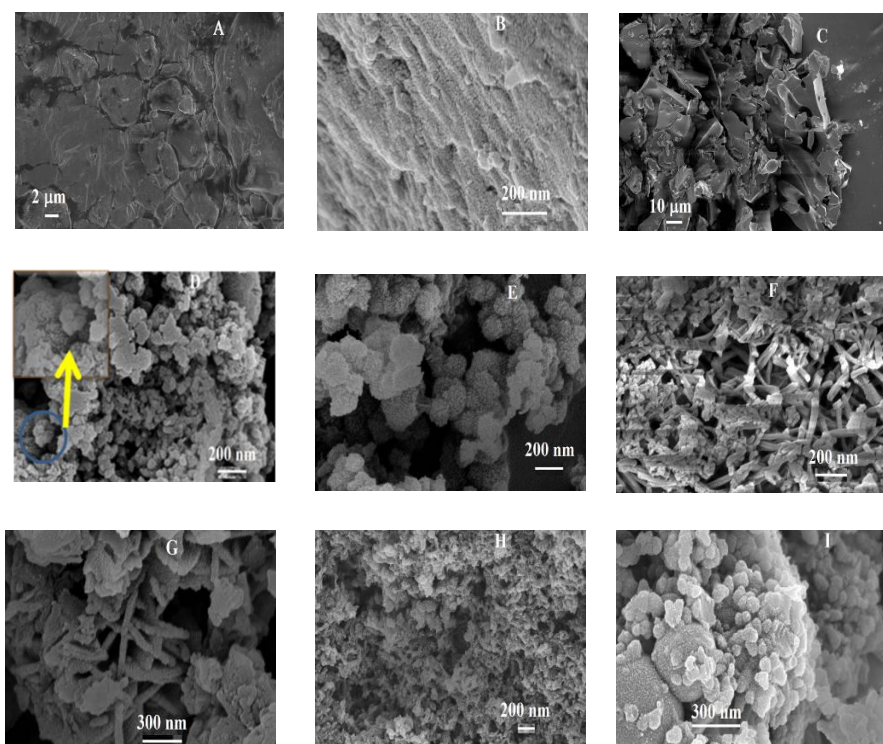


Figure 9. FESEM images of 3-methyl (phenyl amino) propionic acid (A), Poly (3-methyl (phenyl amino) propionic acid) (B), PAA (C), PAA/PANI (PAA : aniline (w/w)=1 : 0.5) composite (D), PAA/PANI (PAA : aniline (w/w)=1 : 0.5) composite (E), AA doped PANI (APS in 1 M HCl) (F), AA doped PANI (APS in 0.5 M HCl) (G), HCl doped PANI (H) and AA doped PANI (APS in water) (I)

X-ray diffraction (XRD) analysis

In this work, X-ray diffraction (XRD) was done to exploit the crystalline/amorphous nature of synthesized AA based PANI polymer. From XRD patterns, AA doped PANI (APS in water), AA doped PANI (APS in 1 M HCl), PAA, PAA/PANI composite and HCl doped PANI are shown in **Fig. 10**. Broad peaks in **Fig. 10** indicate the amorphous nature of the polymer [43]. In case of HCl doped PANI, several diffraction peaks are observed in **Fig. 10**. This shows that PANI chains become more ordered after the doping [44]. On the contrary, two peaks at 19° and 25° are found in the patterns of AA based PANI. It indicates the presence of two polymers (PANI and PAA). This might happen during the polymerization process. Some of the acrylic acid was converted to PAA (polyacrylic acid). Similar pronounced diffraction peaks (at 19° and 25°) of PAA/PANI composite are found in the pattern with high intensity. This indicates the presence of more PAA in the PAA/PANI composite.

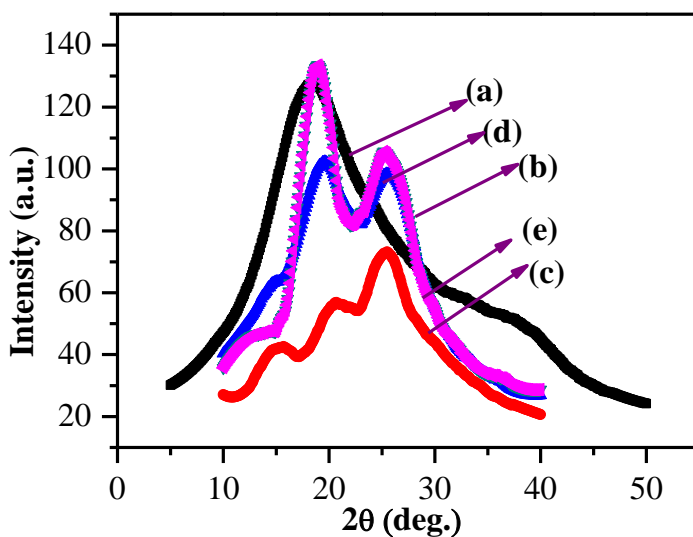


Figure 10. XRD pattern of the PAA (a), PAA/PANI (b), HCl doped PANI (c), AA doped PANI (APS in 1 M HCl) (d) and AA doped PANI (APS in water) (e)

FTIR analysis

FTIR spectra of AA acid based PANI (APS in water), AA acid based PANI (APS in 1 M HCl), poly (3-methyl (phenyl amino) propionic acid), PAA/PANI composite and HCl doped PANI are shown in **Fig. 11**. The different band positions and their assignments are presented in **Table 2**. The most important bands of AA acid doped PANI (APS in water) at 3445 , 2919 , 1550 , 1457 , 1125 and 1269 cm^{-1} have been attributed to N-H, C-H, quinoid, benzenoid, C=N and C-O stretching vibration of acid group, respectively [45]. This indicates that the required characters of the PANI are retained. The main features of AA acid based PANI (APS in 1 M HCl) are found at 3450 , 1595 , 1435 , 1115 , and 2924 cm^{-1} corresponding to N-H, quinoid, benzenoid, C=N stretching and C-H, respectively [45]. From our observation, quinoid (1595

cm^{-1}) and benzenoid ring (1435 cm^{-1}) vibrations are indicated for the AA doped PANI [45]. Also, main bands of prepared poly (3-methyl (phenyl amino) propionic acid) are found at $3450, 1568, 1473, 1120, 2932, 1685, 3681, 1294,$ and 1237 cm^{-1} corresponding to N-H stretching, quinoid, C=C stretching of aromatic ring, C-N stretching, C-H stretching, C=O stretching of acid, O-H stretching and C-O stretching, respectively. The band positions of PAA/PANI composites are found at $3450, 1582, 1491, 1120, 2932, 1710, 3693, 1377,$ and 1288 cm^{-1} for N-H stretching, quinoid stretching, C=C stretching of aromatic ring, C-N stretching, C-H stretching, C=O stretching of acid, O-H stretching and C-O stretching, respectively [46]. The characteristic band positions of HCl doped PANI are found at $3289, 1533, 1453, 1067, 2965, 1375$ and 1262 cm^{-1} for N-H stretching, quinoid stretching, C=C stretching of aromatic ring, C-N stretching, C-H stretching, C=O stretching of acid and C-O stretching, respectively [47].

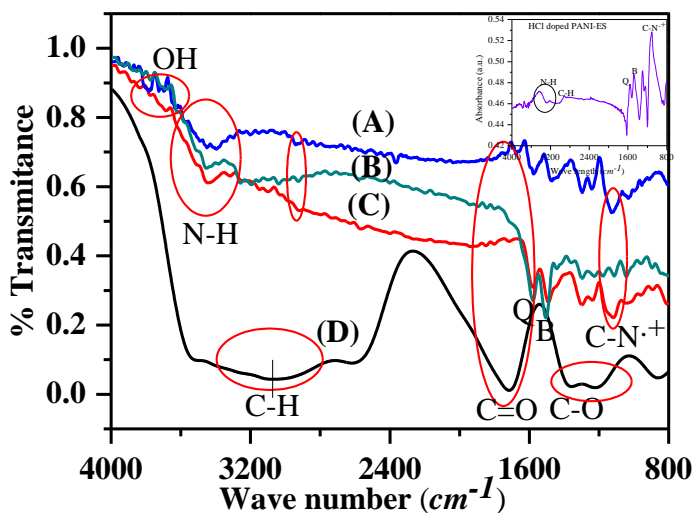


Figure 11. Poly (3-methyl (phenyl amino) propionic acid) (A), AA doped PANI (B), PAA/PANI composite (C), PAA (D)

Table 2. FTIR Peak positions and their assignment of AA doped PANI, Poly (3-methyl (phenyl amino) propionic acid), HCl doped PANI, PAA, PAA/PANI composite

Peak assignments	Peak positions (cm^{-1})				
	AA doped PANI	N substituted PANI	HCl doped PANI	PAA	PAA/PANI composite
NH stretch.	3445	3450	3289	---	3450
Quinoid	1550	1568	1533	---	1582

stretch.					
Benzenoid stretch.	1457	1473	1453	---	1491
C=N stretch.	1125	1120	1067	---	1120
C-H stretch.	2919	2932	2965	3037	2932
C=O stretch.	---	1685	1728	1722	1710
OH stretch.	---	3681	---	---	3693
CH (def.)	---	1294	1375	1364	1377
CH (bending)	1269	1237	1262	1217	1288

H¹NMR analysis

Careful analysis of the H¹NMR characterization of N-substituted PANI polymer [48] obtained from aniline monomer (AA and Ani mixture) product provides insight into the structure of the material. The H¹NMR plot is shown in **Fig. 12**. In the repeat unit, various proton containing groups are presented. The characteristic C-H proton of phenyl ring are found at 6.635-6.915 and 7.019-7.751 ppm, 10 ppm (O-H), 5.740 ppm, and 2.493 and 3.244-3.844 ppm (methylene proton linked to -COOH and -N-), respectively.

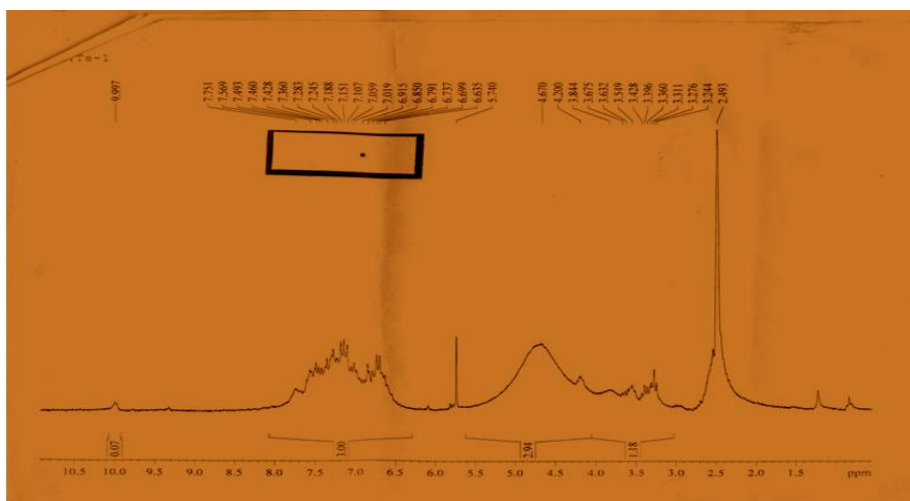


Figure 12. H¹NMR spectrum of N-substituted PANI polymer from acrylic acid and aniline mixture

UV-Visible spectroscopic analysis

It is reported that AA, Ani, 3-methyl (phenyl amino) propanoic acid, poly (3-

methyl (phenyl amino) propanoic acid), AA doped PANI and PAA/PANI composite are shown in **Fig. 13 (a)** and **(b)** in the range (250-800 nm). The type of UV-Visible band positions and their assignments are presented in **Table 3**. The $\pi-\pi^*$ transition was observed at 258 nm due to the presence of π -bond (ethylenic group and C=O) in acrylic acid [49]. The $\pi-\pi^*$ band at 293 nm appeared in the aniline unit [**Fig. 13 (a)**] [50]. Two types of electronic transitions (band) were found at 276 nm and 317 nm in synthesised anilinic monomer (AA and Ani). The assignment may be due to the presence of combined aniline unit and acrylic acid unit in the as prepared salt. This signifies the absence of anilinic unit and excitation band. In the **Fig. 13**, no band is observed in PAA spectrum. PAA/PANI composite shows bands at 272 nm, 294 nm and 564 nm as shown in **Fig. 13 (b)**. The peak observed at 564 nm is due to electronic excitation [46]. This signifies the formation of oxidation state, *i.e.*, salt form of PANI [46]. Also, other two peaks (272 nm, 294 nm) are assigned for $\pi-\pi^*$. These indicate the presence of aniline unit of PANI [46]. As well, AA doped PANI shows two types of bands ($\pi-\pi^*$ and excitation band). This signifies aniline unit and oxidation state of PANI, respectively [51]. Salt forms of PANI contain both amine groups and imine groups. Imine group represents the doped state of PANI, *i.e.*, the N atoms in the imine groups are protonated, N and its neighbouring quinoid ring become a semiquinoid radical cation [52]. The different absorption bands are observed in **Fig. 13 (b)**. This may be happened due to the different rate of doping as well as synthetic procedure [52].

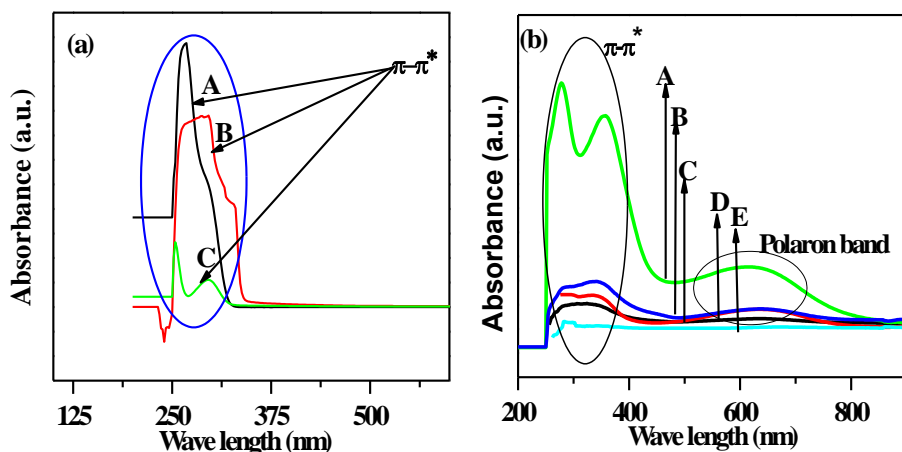


Figure 13. UV-Visible spectra of AA (A), Ani (B), 3-methyl (phenyl amino) propanoic acid (C) in (a), whereas HCl doped PANI (A), AA doped PANI (B), PAA/PANI composites (C), 3-methyl (phenyl amino) propanoic acid (D), and PAA (E) in (b)

Table 3. UV-Visible peak positions and assignments for acrylic acid (AA) based PANI polymers (^aAPS in H₂O, ^bAPS in 1 M HCl)

Peak	Peak positions (nm)
------	---------------------

assignments	AA based PANI ^a	AA doped PANI ^b	HCl doped PANI	N-substituted PANI	PAA/PANI composite
$\pi-\pi^*$	268 & 347	276 & 369	277 & 360	310	338
Polaron band	580	706	614	625	630

The electronic transitions were observed between two bands, which happened after photon absorption. Photon absorption (UV-Visible) semiconductor is followed by Tauc expression [53].

$$(\alpha h\nu) = A (h\nu - E_g)^n \dots\dots\dots (1)$$

Where α = optical absorption co-efficient, $h\nu$ = photon energy, E_g = energy gap calculated from graph, A = absorption constant, n = represents the types of transition. Here, $n = 2$ indicates allowed indirect transitions and $n = 1/2$ indicates allowed direct transitions. The optically (direct) allowed transitions of AA doped PANI, Poly (3-methyl (phenyl amino) propanoic acid), and PAA/PANI composite are shown in **Fig. 13 (c)** and its value is presented in **Table 4**. For direct transition, we can plot $(\alpha h\nu)^2$ vs. $h\nu$ and extrapolate the linear portion of it to $\alpha = 0$ value to obtain

corresponding direct band gap. We estimated two E_g values corresponding to two types of transitions observed from **Fig. 13 (c)**. This band gap values are 3.65 and 2.79 eV for HCl doped PANI, 3.08 eV for PAA/PANI composite, 2.90 eV for AA doped PANI and 2.83 eV for poly (3-methyl (phenyl amino) propanoic acid). There E_g values correspond to the wide band gap of the inorganic semiconductor [53]. This variation is probably due to the formation of PANI polymeric structure using different monomers [53], which means that the different polymeric structures have produced various electronic environments. This environment produces different repulsive electron-electron interactions between two electrons on the same monomer unit or on neighbouring carbons along the backbone. That's why; we got various optical (direct) bands of prepared AA based PANI polymer [54].

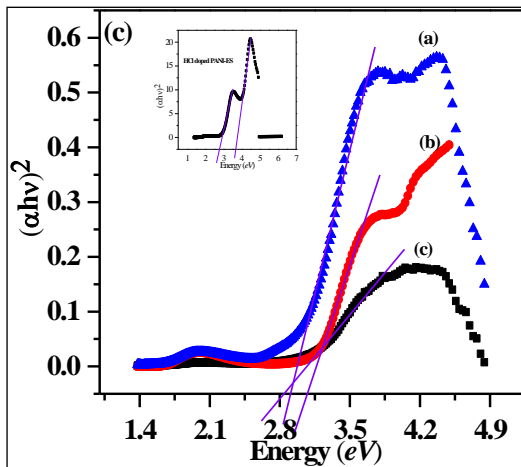


Figure 13(c). Optical (direct) band gap of AA doped PANI (a), PAA/PANI composite (b), poly (3-methyl (phenyl amino) propanoic acid) (c), HCl doped PANI at left corner

DC conductivity

Conductivity is the inherent property of intrinsically conducting polymers (ICPs). To work out the room temperature DC conductivity of using the relation

$\sigma = \frac{1}{\rho}$, where, ρ is resistivity [43]. The resistivity was measured using the relation

$\rho = 2\pi S \left(\frac{V}{I} \right)$, where S is the probe spacing (0.2 cm), I be the applied current in

the four probe system (micro amp regime) and V be the corresponding obtained voltage in (V). At room temperature, the average DC conductivity was found to be 4.79×10^{-4} S/cm for AA doped PANI (APS in water), 0.825 S/cm for AA doped PANI (APS in HCl), 0.135 S/cm for (poly (3-methyl (phenyl amino) propanoic acid) palette), 0.1004 S/cm for PAA/PANI composites, 1.35×10^{-4} S/cm for HCl doped PANI, respectively. The DC conductivity values are indicating the semiconducting material range [43]. The reason may be due to the different strengths of acid dopants as well as monomer unit and that forms different oxidation states in PANI polymer backbone. Dopant helps to extend the conjugation of PANI polymeric structure evolved in the polymerization mechanism. Structural ordering is possible in the polymers and that may be happened due to the incorporation of the charged species [54]. There are signatures supporting these changes in the UV-Vis results. Estimated average DC conductivity at room temperature for AA based PANI is mentioned in **Table 4**.

Table 4. Estimated average DC conductivity at room temperature and optical (direct) band gap of AA based PANI polymer

Parameters	Materials name				
	AA doped PANI ^a	AA doped PANI ^b	Poly (3-methyl (phenyl amino) propanoic acid)	PAA/PANI composite	HCl doped PANI
DC (av.) Conductivity	4.79×10^{-4}	0.8625	0.153	0.1004	1.35×10^{-4}

(S/cm)					
Optical (direct band gap (eV)	2.56 & 3.663	2.90	2.74	3.09	2.82 & 3.76

The variation of DC conductivity with temperature is presented in **Fig. 14(a)** and **(b)** for the prepared materials. It is seen that the conductivity of the prepared materials is increased with the increase of temperature from 70 to 300 K. This behaviour is similar to the behaviour of inorganic semiconductor [25].

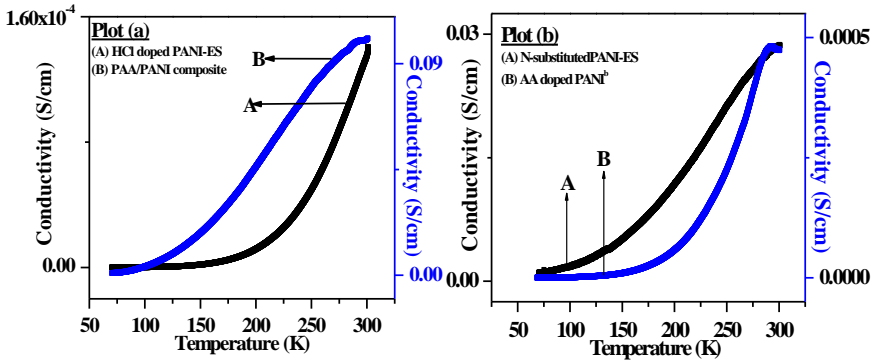


Figure 14. Variation of DC conductivity with temperature of HCl doped PANI (A) and PAA/PANI composite (B) in plot (a), whereas Poly (3-methyl (phenyl amino) propanoic acid (A) and AA doped PANI (APS in 1 M HCl) in plot (b)

DC conductivity of the prepared materials was measured at temperature from 70-300 K in the presence and absence of magnetic field (0.4 T) for better understanding of the conduction mechanism. Several reports have described the metal-insulator (M-I) transition behaviour that occurred in the semiconducting polymeric materials. In this transition, three different regions are identified such as metallic ($\rho_r < 2$), critical ($2 < \rho_r < 6$) and insulating ($\rho_r > 6$) depending on resistivity ratio [28]. Since the resistivity ratio of our prepared materials are more than 2 and then, it is treated as insulating region [28].

Some reports have mentioned about Anderson transition in three dimensional (3D) electronic systems [24]. In this system (3D), fluctuation increases due to random potential. That is why transition occurred from metal to insulator. Because of this transition, the nature of the electron wave functions changes under the influence of the disorder. Particularly in an insulating phase, a potential fluctuation is more and the wave is localised in the region of space [24]. When the Fermi energy lies in a region of localized states and the system is a Fermi glass insulator. In this region, the low temperature transport is possible by variable-range hopping (VRH) [24]. Thermally activated or hopping behaviour is studied by temperature dependent DC conductivity without magnetic field and it is shown in **Fig. 14** (Arrhenius model) and **Fig. 15** (3D VRH model). With the help of Mott's expression (equation 2) and Arrhenius equation,

the more prominent transport behaviour was shown to occur either by thermally activated or hopping process in conducting polymer [25]. Mott’s expression and Arrhenius equation are shown in equation 2 and 3, respectively, whereas R-values are presented in **Table 5**.

$$\sigma = \sigma_0 \exp\left(-\frac{T_0}{T}\right)^r \dots\dots\dots(2)$$

where T_0 is the Mott characteristic temperature and σ_0 the limiting value of conductivity at infinite temperature and the exponent ‘r’ is related to the dimensionality of the transport process via the expression $r = [1/(1+d)]$, where $d = 1, 2$ and 3 for one-, two- and three-dimensional conduction process, respectively.

Arrhenius equation is obtained from rearrangement of Mott’s expression (equation 3). In Arrhenius plot (**Fig. 14**), we plotted $\ln \sigma$ vs $1000/T$.

$$\ln \sigma = \ln \sigma_0 + \left[(-rT_0)\left(\frac{1000}{T}\right)\right] \dots\dots\dots(3)$$

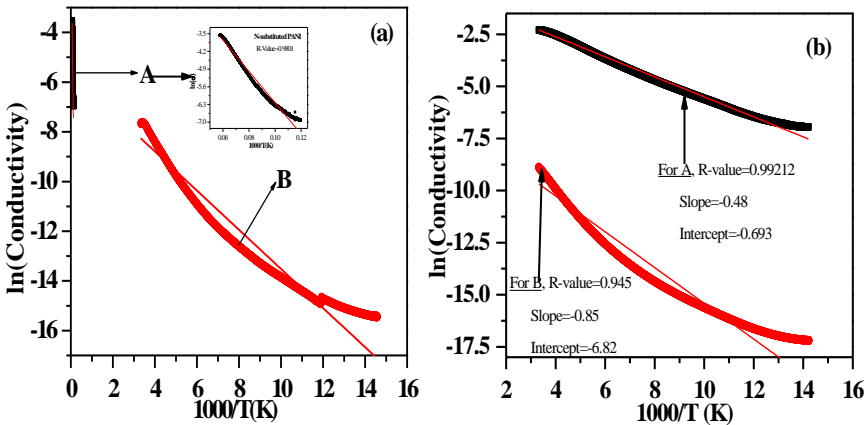


Figure 15. (a): \ln (Conductivity) vs reciprocal Temperature of HCl doped PANI (A) and PAA/PANI composite (B); (b): AA acid doped PANI (APS in 1 M HCl) (A) and poly (3-methyl (phenyl amino) propanoic acid (B)

Arrhenius model (**Fig. 15**) or Mott’s variable range hopping (Mott’s VRH) model (**Fig. 16**) was fitted linearly. The outcomes of regression values are presented in **Table 5**. According to the regression value, the as prepared materials satisfies Mott VRH in three dimensions (3D) except for PAA/PANI composite (followed Mott 1D-VRH). Mott 3D VRH (equation 4) and Mott 1D VRH (equation 5) equations are shown below.

$$\sigma = \sigma_0 \exp\left(-\frac{T_0}{T}\right)^{\frac{1}{4}} \dots\dots\dots(4)$$

$$\sigma = \sigma_0 \exp\left(-\frac{T_0}{T}\right)^{\frac{1}{2}} \dots\dots\dots(5)$$

Table 5. Regression values (R-values) after linear fitting of 3D-VRH, 1D-VRH and Arrhenius model of AA based PANI polymer

Models	Regression values (R-values) of various materials				
	AA doped PANI ^a	AA doped PANI ^b	N-substituted PANI	PAA/PANI composite	HCl doped PANI
VRH (3D) model	0.99048	0.997	0.99508	0.99208	0.99599
VRH (1D) model	0.97859	0.9926	0.99001	0.99712	0.9905
Arrhenius model	0.93928	0.9682	0.97226	0.99212	0.9724

PANI^a: APS in distilled water, PANI^b: APS in 1 M HCl, N-substituted PANI: poly (3-methyl (phenyl amino) propanoic acid

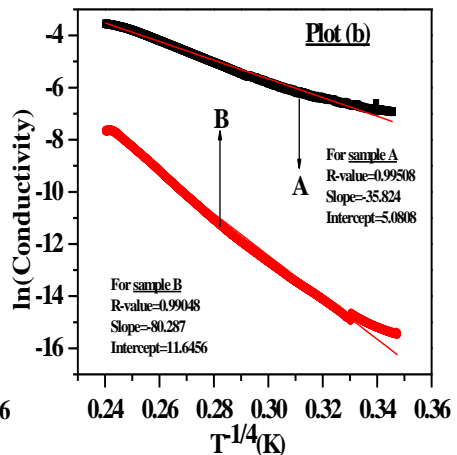
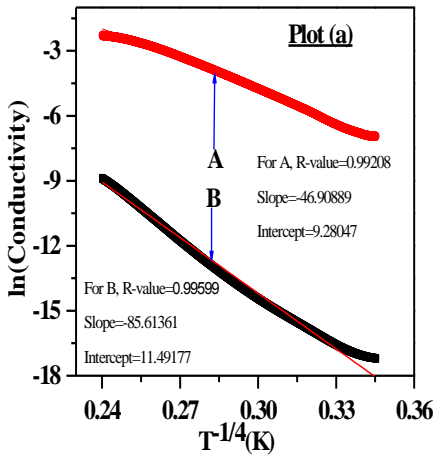


Figure 16. 3D VRH model for temperature variations of DC conductivity of PAA/PANI composite (A) and HCl doped PANI (B) in plot (a), whereas plot (b) Poly (3-methyl (phenyl amino) propanoic acid (A) and AA doped PANI (APS in 1 M HCl) (B) in plot (b)

Since the temperature dependence of DC conductivity is characteristic of variable-range hopping, the densities of states are localized near the Fermi energy. Using Mott’s 3D-VRH (equation 4) and Davis expression (equation 6) and analysing resistivity data, we estimated density of states $[N(E_F)]$ at localised region.

$$T_{Mott} = \frac{16}{[K_B N(E)_F L_{loc}^3]} \dots\dots\dots(6)$$

Where K_B is the Boltzmann constant, $N(E_F)$ is the density of states at the Fermi level, L_{loc} is the localization length [28] and Mott’s temperature. In Mott’s 3D VRH, we plotted $\ln(\text{Conductivity})$ vs. $T^{-1/4}$ and it is fitted linearly. From the slope and intercept of the straight line, we found T_{Mott} and σ_0 which are presented in **Table 6**.

It was reported earlier that possible transitions also occur from the critical regime to insulating regime through variable-range hopping by the application of an external magnetic field [28]. Therefore, magnetic field would be required to achieve the localization of charge carrier [28]. The localization length (L_{loc}) can be done from resistivity data with magnetic field (0.4 T). According to the VRH theory, the resistivity with magnetic field can be expressed as [28]

$$\ln \left[\frac{\rho(H)}{\rho_0} \right] = t (L_{loc} / L_H)^4 \left(\frac{T_{Mott}}{T} \right)^{\frac{3}{4}} \dots\dots\dots(7)$$

Where, $t = 5/2016$, $L_H = (hc/2\pi eH)^{1/2}$ = magnetic length, c = velocity of light (3×10^{10} cm/s), h = Planck’s constant (6.62×10^{-27} erg.sec), e = electronic charge (1.6×10^{-19} C) and $H = 0.4$ T is the applied magnetic field. **Fig. 17** shows the plot of $\ln [\rho(H)/\rho(0)]$ against $T^{-3/4}$ and fitted linearly. From the slope, we estimated the values of L_{loc} and are listed in **Table 6**.

The transport occurs *via* variable-range hopping among localized states on the insulating side of the M-I transition (where $\ln(\text{Conductivity})$ vs $T^{-1/4}$ is a straight line in zero field). By taking the values of T_{Mott} and L_{loc} for each sample from equation (6), the density of state values $[N(E)_F]$ was calculated. The values are presented in **Table 6**. Furthermore, the M-I transition temperature was found from plot of resistivity (ρ) vs temperature (T) and shown in **Fig. 18**. Using T_{Mott} , L_{loc} and M-I transition temperature, we estimated hopping distance ($R_{hop, Mott}$) and hoping energy ($\Delta_{hop, Mott}$), *i.e.*, the energy difference between the sites from the following equations (8) and (9) [28] and mentioned in **Table 6**.

$$\Delta_{\text{hop,Mott}} = \left(\frac{1}{4}\right) (k_B T) \left(\frac{T_{\text{Mott}}}{T}\right)^{\frac{1}{4}} \dots\dots\dots(8)$$

$$R_{\text{hop,Mott}} = \left(\frac{3}{8}\right) \left(\frac{T_{\text{Mott}}}{T}\right)^{\frac{1}{4}} L_{\text{loc}} \dots\dots\dots(9)$$

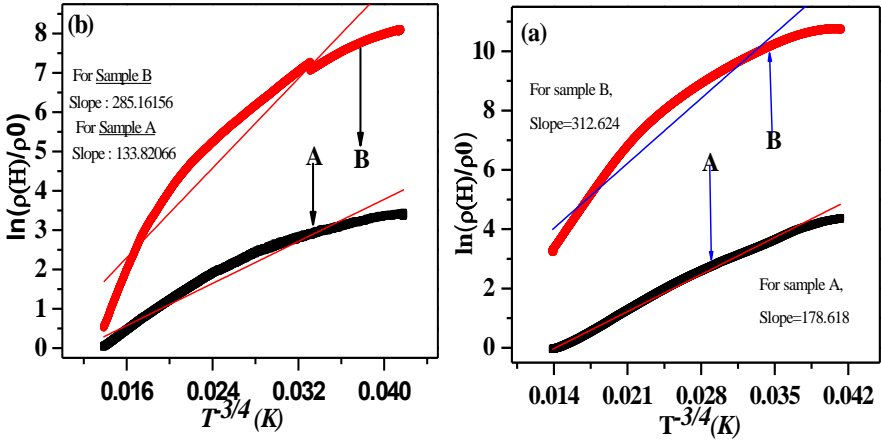


Figure 17 (a). Plots of $[\ln \rho(H)/\rho(0)]$ vs $T^{-4/3}$ for HCl doped PANI (A) and PPA/PANI composite (B) at 0.4 T; (b): Plots of $[\ln \rho(H)/\rho(0)]$ vs $T^{-4/3}$ for poly (3-methyl (phenyl amino) propanoic acid (A) and AA doped PANI (B) at 0.4T with temperature range (70–300 K)

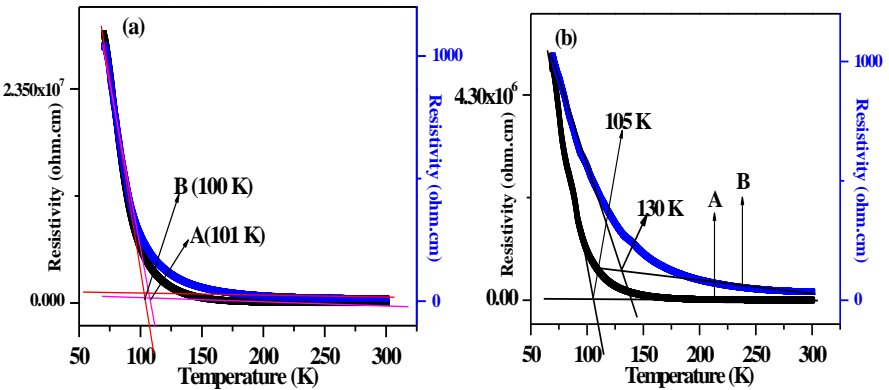


Figure 18:(a). Plots of resistivity (\square) vs temperature (T) for HCl doped PANI (A) and PPA/PANI composite (B); (b): Plots of resistivity (\square) vs temperature (T) for poly (3-methyl (phenyl amino) propanoic acid (A) and AA doped PANI (B) with

temperature range (70-300 K)

From overall results of DC conducting data as a function of temperature, it is concluded that HCl doped PANI shows lower localisation length (L_{loc}) and higher density of states [$N(E_F)$] than other prepared PANI materials presented in this work. That indicates that PANI chains are compacted, *i.e.*, very close to each other. This implies that the wave (electron) is localised more in the region of space in the insulating phase.

Table 6. Conduction parameters obtained by analyzing the low temperature resistivity (with and without magnetic field) data of AA doped PANI

Conducting parameters	N substituted PANI	AA doped PANI ^a	HCl doped PANI	AA doped PANI ^b	PAA/PANI
σ_0	160.9	1.14×10^5	9.79×10^4	1355.6	13.91
M-I transition temp. (K)	144	96	100	125	103
T _{Mott} (K)	1.647×10^6	4.155×10^7	5.37×10^7	8.5×10^5	6.697×10^3
L_{loc} (nm)	231.4	25.49	24.88	40.7496	117.49
N (E_F) (no. states/eV/cm ³)	9.095×10^{18}	2.697×10^{25}	2.244×10^{25}	3.227×10^{21}	1.747×10^{22}
R _{Hop, Mott} (nm)	897.34	245.168	252.73	138.75	124.17
$\Delta_{Hop, Mott}$ (meV)	32.09	53.06	58.37	24.45	6.3
k (eV/K)		8.62×10^{-5}	8.62×10^{-5}	8.62×10^{-5}	8.62×10^{-5}

PANI^a: APS in distilled water, PANI^b: APS in 1 M HCl, N substituted PAN: Poly (3-methyl (phenyl amino) propanoic acid

Thermogravimetric (Tg) Analysis

Fig. 19 shows typical TGA curves of (a) PAA powder (Mol. weight ~1800), (b) PAA/PANI composite, (c) HCl doped PANI (aqueous APS solution), (d) 3-methyl (phenyl amino) propanoic acid, (e) poly (3-methyl (phenyl amino) propanoic acid) and (f) AA doped PANI measured under a nitrogen atmosphere from 28-700 °C. Various

percentages (%) of weight loss are presented in **Table 7**. For PAA powder, the weight losses (about 5 %) before 94°C of these samples are due to losses of adsorbed moisture [55]. The weights of these samples remain unchanged before 185 °C [55]. Total PAA mass is lost at 520 °C and that is observed from **Fig. 19**. From the TGA curve (e) and **Table 7**, it is clear that the PAA/PANI composite film indicates the four stages of weight loss. First stage shows 9 % weight loss due to the loss of moisture and 9 % weight loss occurs in the second stage. This happened due to the loss of HCl molecules. Weight loss at the third stage (7 %) may be due to the loss of low molecular weight PAA. Weight loss at fourth stage (25 %) is due to the decomposition of PANI chain [46,56]. In case of HCl doped PANI, 9 % initial weight loss was observed. This may be happened due to the loss of moisture. PANI chain was lost upto 34 % [57]. 3-methyl (phenyl amino) propanoic acid profile shows two main weight loss steps. It is well known that the first (56 °C) is due to the residual water in the prepared monomer.

Table 7. Thermogravimetric (TG) analyses of 3-methyl (phenyl amino) propanoic acid (monomer), poly (3-methyl (phenyl amino) propanoic acid (polymer), AA doped PANI (APS in water), AA doped PANI (APS in 1 M HCl), PAA, PAA/PANI composite

Different stages (%) of weight loss	N-substituted aniline	N substituted PANI	AA doped PANI ^a	AA doped PANI ^b	PAA	PAA/PANI composite
1 st stage	6	10	12	13	6	9
2 nd stage	75	10	18	11	78	9
3 rd stage	---	5	4	4	---	7
4 th stage	---	20	22	22	---	25
5 th stage	---	5	10	11	---	---

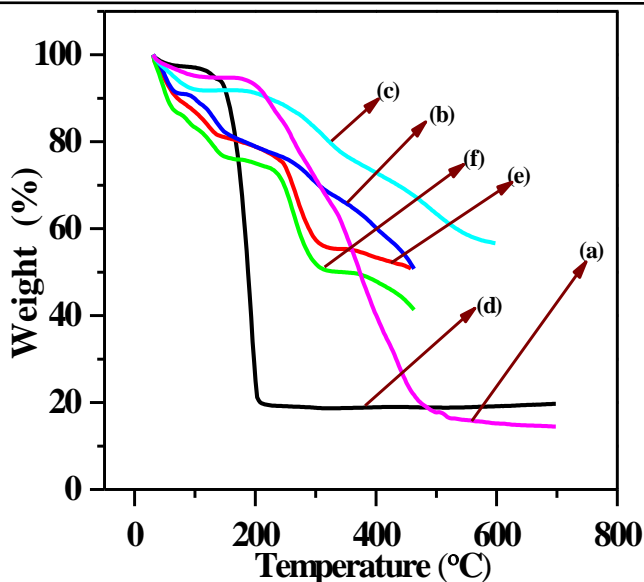


Figure 19. Thermogravimetric (TG) analysis of 3-methyl (phenyl amino) propanoic acid (a), poly (3-methyl (phenyl amino) propanoic acid) (b), AA doped PANI (APS in 1 M HCl) (c), PAA (d), PAA/PANI composite (e) and HCl doped PANI (f)

The second (56–207 °C) indicates the mass loss of the prepared monomer. This loss is attributed to the complete decomposition of the prepared monomer. TGA curve of poly (3-methyl (phenyl amino) propanoic acid) is also shown in **Fig. 19**. Gradual weight losses over the wide temperature in the polymer can be attributed to moisture, HCl, side chains attached to this polymer and finally complete decomposition of PANI polymer which shows better thermal stability than AA doped PANI chain. From overall TGA results, it is concluded that HCl doped PANI (aqueous APS solution) shows better thermal stability than other prepared PANI materials presented in this work.

DSC Analysis

Our major interest was to study the effect of different form of acrylic acid on the thermal behavior of these acrylic acid based PANI and HCl doped PANI. Few reports are found on thermal properties like enthalpy energy and cross-linking temperature of the pristine polyaniline is presented in **Table 8**. Thermal behaviours of the prepared AA based PANI polymeric materials and AA substituted aniline monomer, *i.e.*, 3-methyl (phenyl amino) propanoic acid have been compared with those of HCl doped PANI (aqueous APS solution) was investigated by DSC and plotted in **Fig. 21** for study of enthalpy energy (ΔH). DSC curve of PAA shows two endothermic peaks [55]. The peaks are observed at 172 and 235 °C. At this position, the sample consumes energy values of 98.48 and 48.64 J/g. In addition, the curve

shows two exothermic peaks at 164.38 °C with emitted heat values of 437.1963 J/g, respectively. It signifies the stability of prepared HCl doped PANI polymer [57].

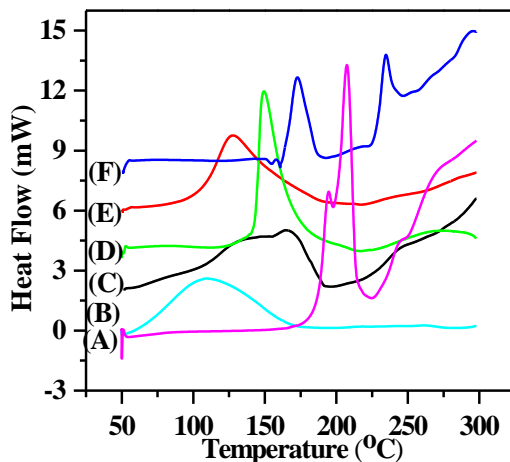


Figure 21. Differential scanning calorimetry (DSC) thermograms of 3-methyl (phenyl amino) propanoic acid (A), poly (3-methyl (phenyl amino) propanoic acid (B), AA doped PANI (APS in water) (C), PAA/PANI composite (D), AA doped PANI (APS in 1 M HCl) (E), and PAA (F)

Table 8. Differential scanning calorimetry (DSC) analyses of 3-methyl (phenyl amino) propanoic acid (monomer), poly (3-methyl (phenyl amino) propanoic acid (polymer), AA doped PANI (APS in water), AA doped PANI (APS in 1 M HCl), PAA, and PAA/PANI composite

Parameters	N-substituted aniline	N substituted PANI	AA doped PANI ^a	AA doped PANI ^b	PAA	PAA/PANI composite
ΔH (J/g)	$\Delta H_1=300.3$ $\Delta H_2=8.02$	$\Delta H_1=345.4$ $\Delta H_2=0$	$\Delta H_1=437.2$ $\Delta H_2=0$	$\Delta H_{11}=236.5$ $\Delta H_2=0$	$\Delta H_1=91.5$ $\Delta H_2=48.6$	$\Delta H_1=251.7$ $\Delta H_2=0$
Temp. at 1 st peak (°C)	207.34	109.86	164.38	127.69	172.66	149.40
Temp. at	243.04	---	---	---	234.58	---

2 nd peak (°C)						
------------------------------	--	--	--	--	--	--

Solubility

Many reports have mentioned the solubility of conducting polymers by incorporation of side chains in the polymer backbone [59-61]. For poly (3-alkylthiophene), both solubility and fusibility have been reached due to the attachment of relatively long, flexible hydrocarbon side groups without changing the π -electronic structure. The qualitative solubility of the N-substituted polymers is summarized in **Table 9**. In contrast to polyaniline (without substitution), N-alkylated polyaniline bearing more than eight carbons of alkylated units already exhibit satisfactory solubilities in different solvents such as chloroform, toluene, THF, and also other common organic solvents. Polyanilines containing longer side chains like PANI-16, and PANI-18, may even be dissolved in hexane and methylene chloride. The main concept is “solvent bound” in the rigid polymers with flexible side chains. In addition, the solubility may affect the stiffness of polymeric chains and that is discussed later. On the other hand, polar solvents such as NMP, DMSO, and DMF are no longer good solvents for these heavily substituted polyanilines because they formed strong hydrogen-bonding interaction and contribute to the dissolution of polyaniline emeraldine base in NMP, DMSO, and m-cresol. Now as a consequence of the side chains, the substituted polyaniline contains the functional groups (-COOH) that can form hydrogen bonding and solvation occurred. In that way their solubility is increased with strong polar solvents. The solubility of the substituted polyaniline depends on the presence of the side chain with a certain concentration as well as the size of the pendant side chain [59-61].

Table 9. Solubility of AA based polyaniline in different solvents

Materials	NMP	DMSO	THF	n-Hexane	Water	CHCl ₃
N-substituted aniline	++	++	++	-	++	++
N-substituted PANI	+	+		-	-	-
AA doped PANI (APS in water)	+	+	+	-	+	-
AA doped PANI (APS in 1 M HCl)	+	+	+	-	+	-
PAA/PANI composite	+	+	+	-	+	-
PANI	+	+	-	-	-	-
PAA	++	++	++	-	++	+

^a Key: ++, well soluble; +, partially soluble; -, slightly soluble or insoluble,

2.4 Response of Liquefied Petroleum Gas (LPG) (i.e., LPG SENSOR)

LPG is one of the flammable gases. It is also called a hazards gas, which is create in both *i.e.*, humans and an environment. It has highly flammable characteristics at ppm level of concentration. It poses a serious threat to humans and an environment. LPG is used in various sectors such as house hold, automotive industries, etc. With the progressive global population, many more peoples are being endangered by the effect due to the exposure of LPG. One of the potential uses of LPG is automotive fuel for vehicles or as a propellant for aerosols. In addition to automotive fuel, of LPG is widely used in cooking. Therefore, it urgent requires detecting precisely, fast and selectively for preventing the occurrence of accidental explosions. Till to date, good LPG sensor has not been found. Now, the problem is vital to industry as well as general public. To meet the requirement, significant research for new sensors is ongoing with enhancing the performance, compared with traditional sensors *i.e.*, resistive metal oxide sensors. Metal oxide based LPG sensors is allowed to detect lower level LPG concentration and their selectivity low. The other important sensor operating parameter is temperature. High temperature is requires for their operation [62-64]. So, power consumption is more, which is reducing the sensor life. Room temperature sensor operation is an important parameter, which is supported to achieve intrinsically safe performance in potentially hazardous situations. This sensors exhibit a fast, reversible response at room temperature [65-67].

In current years, conducting polymer based materials have been used to detect various gas analytes [68-71]. The sensors work on the principle of barrier mechanism [72, 73]. Conversely, LPG response is pronounced at 473 K. For this response, it is required high power consumption and complexities in integration. For meeting the requirements, researchers put their effort to develop new sensor materials. The developed materials are used to analyse LPG gas and other poisoning species. It has better stability, selectivity and lower fabrication costs. The developed novel material is conducting polymer based one *i.e.*, thin films, blends, or heterojunction. Polyaniline is potential member in the conducting polymer family. It is p-type semiconducting material and is used in junction devices [74, 75]. It showed high electrical conductivity in doping state. In the sensor material, I-V characteristic measured the LPG response at different LPG concentration exposure in room temperature. Exposure of LPG gas on sensor materials, current drastically decreased with increase in their concentration. This is due to the change in work function of the polyaniline. Therefore, the resistance of the polyaniline is increased. Hence, current decreases. **Brief summary of LPG gas detection is presented in Table xxx.**

Table. xxx Brief summary of LPG gas detection

Study	Materials	Perporfamce	Optimum temperature (°C)	Limitation
-------	-----------	-------------	--------------------------	------------

Kumar et al. [76]	ZnO/ polyaniline	Response time 25 s	Room Temperature	High LPG concentration
Singh et al. [77]	PANI–Co3O4 nanocomposite	Sensitivity 40%	Room Temperature	High LPG concentration
Taheri et al. [78]	Reduced Graphene Oxide/Gold Nano-hybrid	Response time 5 s	Room Temperature	High LPG concentration
Joshi et al. [79]	n-CdSe/p- polyaniline junction	Response time 50 and 100 s	Room Temperature	High LPG concentration
Dhawale et al. [80]	p-polyaniline/n- TiO2 heterojunction	Response 63 %	Room Temperature	High LPG concentration
Dhawale et al. [81]	n-CdS/p- polyaniline heterojunction	Response 80%	Room Temperature	High LPG concentration

3.0 Conclusions

Flexible PAA/PANI composite was synthesised using chemical oxidation method of aniline in an aqueous solution of PAA. Its morphology and structure show fiber like and amorphous nature. Retaining of chemical groups in the composite backbone is observed from FTIR spectrum. Also, due to the presence of polaron band emeraldine form of PAA/PANI composite is indicated. Room temperature DC conductivity is calculated. Different parameters of conduction mechanism support to understand the transport process. Thermal stability shows better results than HCl doped PANI.

A new bifunctional monomer, *i.e.*, 3-methyl (phenyl amino) propanoic acid incorporating both aniline and acrylic acid, was synthesized and fully characterized. In conjugated poly (3-methyl (phenyl amino) propanoic acid backbone, it is bearing an acrylic acid as side group produced by chemical oxidation polymerization method using ammonium persulfate as oxidant. FTIR, ¹H NMR, and ESI-MS spectroscopic characterizations have supported the prepared 3-methyl (phenyl amino) propanoic acid. FTIR shows the presence of various organic groups in the prepared monomer and polymeric backbone. UV-Visible spectrum indicates the emeraldine form of Poly (3-methyl (phenyl amino) propanoic acid. Calculated average DC conductivity was observed in the semiconducting range. Different transport parameters support to better understand the conduction mechanism. In this study, thermal stability of poly (3-methyl (phenyl amino) propanoic acid shows better results than HCl doped PANI. AA

doped PANI results show feasible data to other AA based PANI polymer. In particular, liquefied petroleum gas responses and mechanism of polyaniline based materials were discussed.

4.0 Acknowledgements

The author conveys their sincere thanks to the CRF, IIT Kharagpur for their providing testing facilities and Materials Science Centre to do the research work. I would like to thank Prof. Debabrat Pradhan for their invaluable guidance, advices, constant inspiration and technical support throughout the entire research program.

5.0 References

- [1] Burroughes, J.H., Bradley, D.D.C., Brown, A.R., Marks, R.N., Mackay, K., Friend, R.H., Burns, P.L., and Homes, A.B. (1990), Light-Emitting Diodes Based on Conjugated Polymers, *Nature*, Vol. 347, pp. 539-541.
- [2] Frackowiak, E., Khomenko, V., Jurewicz, K., Lota, K., and Beguin F. (2006), Supercapacitors Based on Conducting Polymers/Nanotubes Composites, *J. Power Sources*, Vol. 153, pp. 413-418.
- [3] Wu, F., Chen, J., Chen, R., Wu, S., Li, L., Chen, S., and Zhao T. (2011), Sulfur/Polythiophene with a Core/Shell Structure: Synthesis and Electrochemical Properties of the Cathode for Rechargeable Lithium Batteries, *Journal of Physical Chemistry C*, Vol. 115, pp. 6057-6063.
- [4] Yu, L., Jin, X., and Zeng, X. (2008), Methane Interactions with Polyaniline/Butylmethylimidazolium Camphorsulphonate Ionic Liquid Composite, *Langmuir*, Vol. 24, pp. 11631-11636.
- [5] Racicot, R., Brown, R.R., and Yang, S.C. (1997), Corrosion Protection of Aluminium Alloys by Double-strand Polyaniline, *Synthetic Metals*, Vol. 85, pp. 1263-1264.
- [6] Saini, P., Choudhary, V., Vijayan, N., and Kotnala, R. K. (2012), Improved Electromagnetic Interference Shielding Response of Poly(aniline)-Coated Fabrics Containing Dielectric and Magnetic Nanoparticles, *Journal of Physical Chemistry C*, Vol. 116, pp. 13403-13412.
- [7] MacDiarmid, A.G., Chang, J.C., Richter, A.F., and Epstein, A.J. (1987), Polyaniline: a New Concept in Conducting Polymers, *Synthetic Metals*, Vol. 18, pp. 285-290.
- [8] Yue, J., Epstein, A.J., Zhong, Z., Gallagher, P.K., and MacDiarmid, A.G. (1991), Thermal Stabilities of Polyaniline, *Synthetic Metals*, Vol. 41, pp. 765-768.
- [9] Cao, Y., Smith, P., and Heeger, A.J. (1992), Counter-ion Induced

- Processability of Conducting Polyaniline and of Conducting Polyblends of Polyaniline in Bulk Polymers, *Synthetic Metals*, Vol. 48, pp. 91-97.
- [10] Hwang, J.H., and Yang, S.C. (1989), Morphological Modification of Polyaniline Using Polyelectrolyte Template Molecules, *Synthetic Metals*, Vol. 29, pp. 271-276.
- [11] Liu, J.-M., and Yang, S.C. (1991), Novel Colloidal Polyaniline Fibrils Made by Template Guided Chemical Polymerization, *Journal of chemical society, chemical communication*, Vol. 0, pp. 1529- 1531.
- [12] Li, S., Dong, H., and Cao, Y. (1989), Synthesis and Characterization of Soluble Polyaniline, *Synthetic Metals*, Vol. 29, pp. 329 -336.
- [13] Malhotra, B.D., Ghosh, S., and Chandra, R. (1990), Polyaniline/ Polymeric Acid Composite, a Novel Conducting Rubber, *Journal of Applied Polymer Science*, Vol. 40, 1049-1052.
- [14] Kang, Y., Lee, M.-H., and Rhee, S.B. (1992), Electrochemical Properties of Polyaniline Doped with Poly(styrenesulfonic acid), *Synthetic Metals*, Vol. 52, pp. 319-328.
- [15] Lapkowski, M. (1993) Electrochemical Synthesis of Polyaniline/ Poly (2-acryl-amido-2- methyl-1-propane-sulfonic acid) Composite, *Synthetic Metals*, Vol. 55-57, pp. 1558-1563.
- [16] Angelopoulos, M., Patel, N., and Saraf, R. (1993), Amic Acid Doping of Polyaniline: Characterization and Resulting Blends, *Synthetic Metals*, Vol. 55-57, pp. 1552-1557.
- [17] Angelopoulos, M., Patel, N., Shaw, J.M., and Labianca, N.C. 1994, Water Soluble Polyanilines: Properties and Applications, *Materials Research Society Symposium Proceeding*, Vol. 328, pp. 173-xxx.
- [18] Angelopoulos, M., Patel, N., Shaw, J.M., Labianca, N.C., and Rishton, S.A. (1993), Water Soluble Conducting Polyanilines: Applications in Lithography, *Journal of Vacuum Science and Technology B*, Vol. 11(6), pp. 2793-2191.
- [19] Chevalier, J.-W., Bergeron, J.-Y., and Dao, L.H. (1992), Synthesis, Characterization, and Properties of Poly (N-alkylanilines), *Macromolecules*, Vol. 25, pp. 3325-3331.
- [20] Wei, Y., Focke, W.W., Wnek, G.E., Ray, A., and MacDiarmid, A.G. (1989), Synthesis and Electrochemistry of Alkyl Ring-Substituted Polyanilines, *Journal of Physical Chemistry*, Vol. 93, pp. 495-499.
- [21] Wei, Y., Hariharan, R., and Patel, S.A. (1990), Chemical and Electrochemical Copolymerization of Aniline with Alkyl Ring-Substituted Anilines, *Macromolecules*, Vol. 23, pp. 158-164.

-
- [22] Bergeron, J.-Y., and Dao, L.H. (1992), Electrical and Physical Properties of New Electrically Conducting Quasi Composites. Poly (aniline-co-N-butylaniline) copolymers, *Macromolecules*, Vol. 25, pp. 3332-3337.
- [23] Cao, Y., Smith, P., and Heeger, A.J. (1993), Counter-ion Induced Processibility of Conducting Polyaniline, *Synthetic Metals*, Vol. 55-57, pp. 3514-3519.
- [24] Menon, R., Yoon, C.O., Moses, D., Heeger, A.J., and Cao, Y. (1993), Transport in Polyaniline near the Critical Regime of the Metal-insulator Transition, *Physical Review B: Condensed Matter*, Vol. 48, pp. 17685-17694.
- [25] Li, J., Fang, K., Qiu, H., Li, S., and Mao, W. (2004), Micromorphology and Electrical Property of the HCl-doped and DBSA-doped Polyaniline, *Synthetic Metal*, Vol. 142, pp. 107-111.
- [26] Kapil, A., Taunk, M., and Chand, S. (2010), Preparation and Charge Transport Studies of Chemically Synthesized Polyaniline, *Journal of Materials Science: Materials in Electronics*, Vol. 21 pp. 399-404.
- [27] Mukherjee, A.K., and Reghu, M. (2005), Magnetotransport in Doped Polyaniline, *Journal of Physics: Condensed Matter*, Vol. 17, pp. 1947-1960.
- [28] Ghosh, M., Barman, A., De, S.K., and Chatterjee, S. (1998), Electrical Resistivity and Magnetoresistivity of Protonic Acid (H₂SO₄ and HCl)-Doped Polyaniline at Low Temperature, *Journal of Applied Physics*, Vol. 84, pp. 806-811.
- [29] Aleshin, A.N., Mironkov, N.B., Suvorov, A.V., Conklin, J.A., Su, T.M., and Kaner, R. B. (1996), Transport Properties of Ion-implanted and Chemically Doped Polyaniline Films, *Physics Review B*, Vol. 54, pp. 11638-11643.
- [30] Tzamalīs, G., Zaidi, N.A., and Monkman, A.P. (2003), Applicability of the Localization-interaction Model to Magnetoconductivity Studies of Polyaniline Films at the Metal-insulator Boundary, *Physics Review B*, Vol. 68, pp. 245106-245111.
- [31] Long, Y., Chen, Z., Wang, N., Li, J., and Wan, M. (2004), Electronic Transport in PANI-CSA/PANI-DBSA Polyblends, *Physica B*, Vol. 344, pp. 82-87.
- [32] Yoon, C.O., Reghu, M., Moses, D., and Heeger, A.J. (1994), Transport near the Metal-insulator Transition: Polypyrrole Doped with PF₆, *Physics Review B*, Vol. 49, pp. 10851-10863.
- [33] Sutar, D., Mithra, M., Reghu, M., and Subramanyam, S.V. (2001), Conductivity and Magnetoresistance in Polypyrrole-PF₆ at Various Doping Level, *Synthetic Metal*, Vol. 119, pp. 455-456.
- [34] Chauvet, O., Paschen, S., Forro, L., Zuppiroli, L., Bujard, P., Kai, K., and

- Wernet, W. (1994), Magnetic and Transport Properties of Polypyrrole Doped with Polyanions, *Synthetic Metal*, Vol. 63, pp. 115-119.
- [35] Aleshin, A.N., Kiebooms, R., Reghu, M., and Heeger, A.J. (1997), Electronic Transport in Doped Poly (3,4-ethylenedioxythiophene) Near the Metal-insulator Transition, *Synthetic Metal*, Vol. 90, pp. 61-68.
- [36] Joseph, T., Shanbhag, G.V., Sawant, D.P., and Halligudi, S.B. (2006), Chemoselective anti-Markovnikov Hydroamination of σ,β -Ethylenic Compounds with Amines using Montmorillonite Clay, *Journal of Molecular Catalysis A: Chemical*, Vol. 250, pp. 210-217.
- [37] Gene, H.-S., Hugh, C.-M., and Christopher, B.-K. (2008) Living Star Polymer Formation: Detailed Assessment of Poly (acrylate) Radical Reaction Pathways via ESI-MS, *Macromolecules*, Vol. 41, pp. 3023-3041.
- [38] Zheng, L., Zhang, S., Yu, X., Zhao, L., Gao, G., Yang, X., Duan, H., and Cao, S. (2006), Enhancement of Enantioselectivity in Lipase-Catalyzed Resolution of N-(2-Ethyl-6-Methylphenyl) Alanine by Additives, *Journal of Molecular Catalysis B: Enzymatic*, Vol. 38, pp. 17-23.
- [39] Cambridge Isotope Laboratories, Inc. 50 Frontage Road, Andover MA 01810, NMR Solvent Data Chart.
- [40] Max, J.-J., and Chapados, C. (2004), Infrared Spectroscopy of Aqueous Carboxylic Acids: Comparison between Different Acids and Their Salts, *J. Phys. Chem. A*, Vol. 108, pp. 3324-3337.
- [41] Ilic, M., Koglin, E., Pohlmeier, A., Narres, H.D., and Schwuger, M.J. (2000), Adsorption and Polymerization of Aniline on Cu (II)-Montmorillonite: Vibrational Spectroscopy and ab Initio Calculation, *Langmuir*, Vol. 16, pp. 8946-8951.
- [42] Sridevi, D., and Rajendran, K.V. (2009), Synthesis and Optical Characteristics of ZnO nanocrystals, *Bulletin of Materials Science*, Vol. 32, pp. 165-168.
- [43] Sengupta, P.P., Kar, P., and Adhikari, B. (2009), Influence of Dopant in the Synthesis, Characteristics and Ammonia Sensing Behavior of Processable Polyaniline, *Thin Solid Films*, Vol. 517, pp. 3770-3775.
- [44] Pawar, S.G., Patil, S.L., Chougule, M.A., Achary, S.N., and Patil, V.B. (2011), Microstructural and Optoelectronic Studies on Polyaniline: TiO₂ Nanocomposites, *International Journal of Polymeric Materials*, Vol. 60, pp. 244-254.
- [45] Athawale, A.A., and Chabukswar, V.V. (2001), Acrylic Acid-Doped Polyaniline Sensitive to Ammonia Vapors, *Journal of Applied Polymer Science*, Vol. 79, pp. 1994-1998.
- [46] Chen, S.-A., and Lee, H.-T. (1995), Structure and Properties of Poly (acrylic

- acid)-Doped Polyaniline, *Macromolecules*, Vol. 28, pp. 2858-2866.
- [47] Liu, R., Qiu, H., Zong, H., and Fang, C. (2011), Fabrication and Characterization of Composite Containing HCl-Doped Polyaniline and Fe Nanoparticles, *Journal of Nanomaterials*, Vol. 2012, pp. 1-8.
- [48] Kavitha, B., Prabakar, K., Kumar, K.S., Srinivasu, D., Srinivas, Ch., Aswal, V.K., Siriguri, V., and Narsimlu, N. (2012), Spectroscopic Studies of Nano Size Crystalline Conducting Polyaniline, *IOSR Journal of Applied Chemistry (IOSRJAC)*, Vol. 2, pp. 16-19.
- [49] Chabukswar, V., and Bhavsar, S. (2010), Synthesis and characterization of organically soluble and electrically conducting acids doped polyaniline, *Chemistry and Chemical Technology*, Vol. 4, pp. 277-280.
- [50] Valle, M.A.D., Gacitúa, M.A., Borrego, E.D., Zamora, P.P., Díaz, F.R., Camarada, M.B., Antilén, M.P., and Soto, J.P. (2012), Electro-Synthesis and Characterization of Aniline and o-Anisidine Oligomers, *International Journal of Electrochemical Science*, Vol. 7, pp. 2552-2565.
- [51] Athawale, A.A., Kulkarni, M.V., and Chabukswar, V.V. (2002), Studies on Chemically Synthesized Soluble Acrylic Acid Doped Polyaniline, *Materials Chemistry and Physics*, Vol. 73, pp. 106-110.
- [52] Furukawa, Y., Ueda, F., Hyodo, Y., Harada, I., Nakajima, T., and Kawagoe, T. 1988, Vibrational Spectra and Structure of Polyaniline, *Macromolecules*, Vol. 21, pp. 1297-1305.
- [53] Sajeev, U.S., Mathai, C.J., Saravanan, S., Ashokan, R.R., Venkatachalam, S., and Anantharaman, M. R. (2006), on the Optical and Electrical Properties of rf and a.c. Plasma Polymerized Aniline Thin Films, *Bulletin of Materials Science*, Vol. 29, pp. 159-163.
- [54] Patil, A.O., Heeger, A.J., and Wudl, F. (1988), Optical Properties of Conducting Polymers, *Chemistry Review*, Vol. 88, pp. 183-200.
- [55] Moharram, M.A., and Allam, M.A. (2007), Study of the Interaction of Poly (acrylic acid) and Poly (acrylic acid)-Poly (acrylamide) Complex with Bone Powders and Hydroxyapatite by Using TGA and DSC, *Journal of Applied Polymer Science*, Vol. 105, pp. 3220-3227.
- [56] HAN, M.G., and IM, S.S. (1999), Electrical and Structural Analysis of Conductive Polyaniline/Polyimide Blends, *Journal of Applied Polymer Science*, Vol. 71, pp. 2169-2178.
- [57] Gomes, E.C., and Oliveira, M.A.S. (2012), Chemical Polymerization of Aniline in Hydrochloric Acid (HCl) and Formic Acid (HCOOH) Media. Differences between the Two Synthesized Polyanilines, *American Journal of Polymer Science*, Vol. 2, pp. 5-13.
- [58] Cardoso, M.J.R., Lima, M.F.S., and Lenz, D.M. (2007), Polyaniline

- Synthesized with Functionalized Sulfonic Acids for Blends Manufacture, *Materials Research*, Vol. 10, pp. 425-429.
- [59] Zheng, W.-Y., Levon, K., Laakso, J., and Bterholm, J.-E. (1994), Characterization and Solid-state Properties of Processable N-Alkylated Polyaniline in the Neutral State, *Macromolecules*, Vol. 27, pp. 7754-7768.
- [60] Bergeron, J.-Y., Chevalier, J.-W., and Dao, L.H. (1990), Water-soluble Conducting Poly (ani line) Polymer, *Journal of Chemical Society: Chemical Communications*, Vol. xxx, pp. 180-182.
- [61] Kim, Y.H., and Calabrese, J.C. (1991), N-Alkylated Aromatic Polyamides, *Macromolecules*, Vol. 24, pp. 2951-2954.
- [62] More, A.M., Gunjakar, J.L., and Lokhande, C.D. 2008, Liquefied Petroleum Gas (LPG) Sensor Properties of Interconnected Web-Like Structured Sprayed TiO₂ Films, *Sensor and Actuators B*, Vol. 129 pp. 671-677.
- [63] Gunjakar, J.L., More, A.M., and Lokhande, C.D. 2008, Chemical Deposition of Nanocrystalline Nickel Oxide from Urea Containing Bath and its Use in Liquefied Petroleum Gas Sensor, *Sensor and Actuators B*, Vol. 131, pp. 356-361.
- [64] Salunkhe, R.R., Shinde, V.R., and Lokhande, C.D. 2008, Liquefied Petroleum Gas (LPG) Sensing Properties of Nanocrystalline CdO Thin Films Prepared by Chemical Route:Effect of Molarities of Precursor Solution, *Sensor and Actuators B*, Vol. 133, 296-301.
- [65] Fang, Q., Chetwynd, D.G., Covington, J.A., Toh, C.S., and Gardner, J.W. 2002, Microgas-Sensor with Conducting Polymers, *Sensor and Actuators B*, Vol. 84, pp. 66-71.
- [66] Xie, D., Jiang, Y., Pan, W., Li, D., Wu, Z., and Li, Y. 2002, Fabrication and Characterization of Polyaniline-based Gas Sensor by Ultra-Thin Film Technology, *Sensor and Actuators B*, Vol. 81, pp. 158-164.
- [67] Zee, F., and Judy, J.W. 2001, Micromachined Polymer-based Chemical Gas Sensor Array, *Sensor and Actuators B*, Vol. 72, pp. 120-128.
- [68] Traversa, E., Miyayama, M., and Yanagida, H. 1994, Gas Sensitivity of ZnO/La₂CuO₄ Heterocontacts, *Sensor and Actuators B*, Vol. 17, pp. 257-261.
- [69] Tamaki, J., Maekawa, T., Miura, N., and Yamazoe, N. 1992, CuO-SnO₂ Element For Highly Sensitive and Elective Detection of H₂S, *Sensor and Actuators B*, Vol. 9, pp. 197-203.
- [70] Zhou, X., Cao, Q., Hu, Y., Gao, J., and Xu, Y. 2001, Sensing Behavior and Mechanism of La₂CuO₄-SnO₂ Gas Sensors, *Sensor and Actuators B* Vol. 77, pp. 443-446.
- [71] Zhou, X., Cao, Q., Huang, H., Yang, P., and Hu, Y. 2003, Study on Sensing

- Mechanism of CuO-SnO₂ Gas Sensors, *Materials Science & Engineering B*, Vol. 99, pp. 44-47.
- [72] Hikita, K., Miyayama, M., and Yanagida, H. 1995, New Approach To Selective Semiconductor Gas Sensors using a de-based PN Heterocontact, *Journal of American Ceramic Society*, Vol. 78, pp.865-873.
- [73] Ling, Z., Leach, C., and Freer, R.2003, NO₂ Sensitivity of a Heterojunction Sensor based on WO₃ and Doped SnO₂, *Journal of European Ceramic Society*, Vol. 23, pp. 1881-1891.
- [74] Narasimhan, M., Hagler, M., Cammarata, V., and Thakur, M. 1998, Junction Devices based on Sulfonated Polyaniline, *Applied Physics Letter*, Vol. 72, pp. 1063-1065.
- [75] Xu, B., Ovchencov, Y., Bai, M., Caruso, A.N., Sorokin, A.V., Ducharme, S., Doudin, B., and Dowben, P.A. 2002, Heterojunction Diode Fabrication from Polyaniline and a Ferroelectric Polymer, *Applied Physics Letter*, Vol. 81, pp. 4281-4283.
- [76] Kumar, S., Kumar, L., and Sharma, V.K. 2020, Synthesis of ZnO/polyaniline Nanocomposite and its Application as Liquefied Petroleum Gas Sensor, *International Journal on Emerging Technologies*, Vol. 11, pp. 419-424.
- [77] Singh, N. Singh, P.K., Singh, M., Gangopadhyay, D., Singh, S.K., and Tandon, P. 2019, Development of a Potential LPG Sensor based on a PANI-CoO Nanocomposite that Functions at Room Temperature, *New Journal of Chemistry*, Vol. 43, pp. 17340-17350.
- [78] Taheri, M., Feizabadi, Z., and Mansour, N. Fast Response and High Sensitivity of Reduced Graphene Oxide/Gold Nano-hybrid for LPG Sensors at Room Temperature, *Journal of Electronic Materials*, vol.xxx, year, pp.
- [79] Joshi, S.S., Lokhande, C.D., and Han, S.-H. 2007, A Room Temperature Liquefied Petroleum Gas Sensor based on all-Electrodeposited n-CdSe/p-Polyaniline Junction, *Sensors and Actuators B*, Vol. 123, pp. 240-245.
- [80] Dhawale, D.S., Salunkhe, R.R., Patil, U.M., Gurav, K.V., More, A.M., and Lokhande, C.D. 2008, Room Temperature Liquefied Petroleum Gas (LPG) Sensor based on p-Polyaniline/n-TiO₂ Heterojunction, *Sensors and Actuators B*, Vol. 134, pp. 988-992.
- [81] Dhawale, D.S., Dubala, D.P., Jamadadea, V.S., Salunkhea, R.R., Joshi, S.S., and Lokhande, C.D. 2010, Room Temperature LPG Sensor based on n-CdS/p-Polyaniline Heterojunction, *Sensors and Actuators B* Vol. 145, pp. 205-210.